6-1991

Double Ionization of Helium by Intermediate to High Velocity He^+ Projectiles

Jun Forest
Western Michigan University

DOUBLE IONIZATION OF HELIUM BY INTERMEDIATE TO HIGH VELOCITY HE^+ PROJECTILES

by

Jun Forest

A Thesis
Submitted to the
Faculty of The Graduate College
in partial fulfillment of the
requirements for the
Degree of Master of Arts
Department of Physics

Western Michigan University
Kalamazoo, Michigan
June 1991

DOUBLE IONIZATION OF HELIUM BY INTERMEDIATE TO HIGH VELOCITY HE^+ PROJECTILES

Jun Forest, M.A.

Western Michigan University, 1991

Ionization of helium target atoms by He^+ projectiles colliding with helium at energies of 0.125 to 3.0 MeV/u is investigated. Cross sections for single and double ionization, and ratios of double-to-single ionization are determined for each outgoing projectile charge state, and are compared to previous studies. For the lowest energies investigated, the ratios are consistent with the two-step mechanism in which the projectile interacts separately with each target electron. At the highest energies, the ratios reach nearly constant values indicating approach to the high velocity limit. At these high energies, however, the ratios are all higher than the value predicted by the empirical equation of Knudsen et al. (1984). Furthermore, the constant ratios in the high velocity limit are strongly dependent on the outgoing projectile charge state indicating different amount of electron correlation being responsible for double ionization associated with projectile capture, loss, or no charge change, respectively.

ACKNOWLEDGMENTS

I wish to express my sincere appreciation to my advisor, Dr. John A. Tanis, for his patience, guidance and encouragement throughout this project. My work with Dr. Tanis allowed me to realize my full potential and exceed my own expectations, leaving me with the abilities necessary for a successful career in physics. My thanks also go to Dr. Steve Ferguson for operating the accelerator, on which this experiment was performed, and Dr. Roger Haar for the many discussions concerning the electronics involved in this work.

I would also like to thank the members of my committee, Dr. Emanual Kamber and Dr. Alvin Rosenthal, for their valuable suggestions and comments offered concerning this work.

Very special thanks go to my husband, Tony Forest, for his love, understanding, patience and support during the years of my study.

Jun Forest

Order Number 1344710

Double ionization of helium by intermediate to high velocity He^+ projectiles

Forest, Jun, M.A.

Western Michigan University, 1991

U·M·I
300 N. Zeeb Rd.
Ann Arbor, MI 48106

TABLE OF CONTENTS

LIST OF TABLES

LIST OF FIGURES

List of Figures—Continued

CHAPTER I

INTRODUCTION

In an ion-atom collision, one of the basic processes is ionization caused by the Coulomb forces between the interacting particles. Ionization involving one electron (single ionization) is well understood, especially at high collision velocities where the independent electron approximation (IEA) can be used to describe the collision process (McGuire & Weaver, 1977; Sidorovitch & Nikolaev, 1983). Ionization processes involving two electrons (double ionization), however, are more complicated due to the fact that the Coulomb interaction between the electrons may not be negligible compared with the interactions between the nuclei and the electrons. Therefore double ionization can depend sensitively on the electron-electron interaction.

The electron-electron interaction can give rise to ionization via direct impact or via electron correlation. Electron correlation can be studied by observing deviations from the independent-particle picture. Theoretically, electron correlation has been defined as the difference between the exact two-electron probability amplitude and the independent-particle amplitude (McGuire, 1987). Furthermore, McGuire (1987) divided electron correlation into two types: static and scattering correlation. Static correlation is contained in the asymptotic wave functions and is dominant in the limit of high collision velocities, while scattering correlation occurs during the collision and is important at lower velocities.

An important collision process which can be used to study correlation effects is the double ionization of helium by fast projectile ions. The reasons are, first, that the helium atom contains just two electrons; second, due to the small nuclear charge,

electron-electron interactions can give rise to relatively large effects in the double-ionization cross section; third, for high ion velocity, v, and low ion charge, q, double ionization is expected to be almost entirely due to electron correlation. Electron correlation effects have considerable importance for the understanding of many-body problem, and have been investigated by various groups both theoretically (Mittleman, 1966; Byron & Joachain, 1966; McGuire, 1982, 1984, 1987; Reading & Ford, 1987) and experimentally (Knudsen et al., 1984; Andersen et al., 1986, 1987; Shah & Gilbody, 1985; DuBois & Toburen, 1988; Tanis et al., 1989; Heber, Bandong, Sampoll, & Watson, 1990). Furthermore, an understanding of the collision processes is important for research in other fields such as plasma physics (Drawin, 1980) and astrophysics (Steigman, 1975).

The projectile charge q and impact velocity v are the two important parameters in understanding the interaction mechanisms. It is well known that single ionization of atoms by fast ions can be satisfactorily described within the independent-electron model using the first Born approximation (Inokuti, 1971; Madison & Merzbacher, 1972). Double ionization, however, can depend sensitively on electron correlation. It was first proposed by McGuire (1982) that double ionization by ions at high velocities ($v_{ion} > 10\ v_{Bohr}$) can be understood in terms of two mechanisms: (1) a two-step process (TS), second order in q/v, in which both target electrons are removed in separate direct interactions with the projectile, and (2) a shakeoff process (SO), first order in q/v, in which the first electron is removed in a direct interaction with the projectile while the second electron is ejected when the resulting ion relaxes to a continuum state. The former process involves independent-particle interactions and is dominant at lower projectile energies, while the latter is due to electron correlation and is dominant at higher projectile energies. Since the parameter q/v is a key factor in characterizing the

ionization cross sections, studying the velocity (or energy) dependence and charge dependence of double ionization of helium can provide an insight into the relative importance of these two competing mechanisms in different q/v ranges. Several experiments on the double ionization of helium have been performed for various projectiles with different charges and over large projectile energy ranges (Knudsen et al., 1984, with various projectiles of charge 1-8 and energy 0.13-15 MeV/u; Shah & Gilbody, 1985, H^+, He^{2+}, Li^{3+} with energies 0.05-2.38 MeV/u; Andersen et al., 1986, p and p^-, with energies 0.1-10 MeV for p, and 0.5-4.1 MeV for p^-; Wood, Edwards, & Ezell, 1986, He^+ with energies 0.025-0.75 MeV/u; Tanis et al., 1987, $O^{5,6,7,8+}$ with energies 0.5-1.5 MeV/u; Heber et al., 1990, N^{7+} with energies 10-30 MeV/u).

Double ionization of helium can occur via: (a) pure ionization in which the projectile charge is unchanged, (b) associated single electron capture by the projectile, and (c) associated single electron loss from the projectile. For pure ionization, the impact parameter is large enough so that the projectile charge is unaffected by the collision. On the other hand, target ionization accompanied by electron capture or loss must occur at smaller impact parameters such that the projectile can capture or lose an electron. Thus, the study of the double ionization of helium associated with electron capture, electron loss, or no charge change can be useful in understanding the dependence of this process on the impact parameter.

The purpose of this work is to study the double ionization of helium by He^+ projectiles. Double ionization of helium by fully stripped ions has been investigated quite extensively and is fairly well understood (Knudsen et al., 1984, 1987; Shah & Gilbody, 1985, H^+, He^{2+}, Li^{3+}), whereas double ionization by partially stripped ions (He^+ here) is much more complicated due to the projectile electron(s) and has not been conclusively studied. The study of double ionization of helium by He^+ ions as

compared with that by fully stripped ions can give information about how the projectile electron affects the interaction, and therefore give us more insight into the many-body problem. Previous experiments with He^+ on He were performed only at low projectile energies (Wood et al., 1986, with energies 0.025-0.75 MeV/u; DuBois & Toburen, 1988, with energies 0.033-0.5 MeV/u); no information is available at high energies for He^+ projectile. In order to investigate double ionization for different ranges of impact parameters, and to examine the relative importance of the two-step and shakeoff mechanisms in these different ranges, we have measured the single and double ionization of helium by He^+ ions undergoing electron capture, electron loss, or no charge change over a large projectile energy range (from 0.125 to 3 MeV/u). Measurements were also carried out for He^{2+} projectiles with energies 0.5, 1, and 1.5 MeV/u. Measured cross sections are compared with various scaling rules from different investigators. Ratios of double-to-single ionization associated with electron capture, electron loss, and no charge change are obtained and compared with previous studies. High-velocity limits for the double-to-single ionization ratio are deduced and compared with the high-energy photoionization ratio.

In the next chapter, the theoretical description is given. The experimental procedure is discussed in detail in Chapter III, and the data analysis techniques are presented in Chapter IV. In Chapter V, the results are presented in tables as well as displayed in graphs, and comparisons of the present results with previous studies are made. Finally, the conclusions are given in Chapter VI.

CHAPTER II

THEORETICAL DESCRIPTION

When an ion of sufficient energy collides with a target atom, one of the many different processes which may take place is ionization of the target. In the past decade, there has been much research on the ionization of target atoms by different projectile ions (Inokuti, 1971; Madison & Merzbacher, 1972; Haugen et al., 1982; Knudsen et al., 1984). Of interest here is the ionization of helium by He^+ projectiles.

When a fast He^+ projectile collides with a helium target atom, single and double ionization of the He target accompanied by projectile electron capture, loss, or no charge change may occur. The general processes are described below:

Single ionization of He accompanied by no projectile charge change (or pure single ionization):

$$He^+ + He \text{ -------- } He^+ + He^+ + e^- \quad (1)$$

Double ionization of He accompanied by no projectile charge change (or pure double ionization):

$$He^+ + He \text{ -------- } He^+ + He^{2+} + 2e^- \quad (2)$$

Single ionization of He by projectile electron capture:

$$He^+ + He \text{ -------- } He + He^+ \quad (3)$$

Double ionization of He by simultaneous electron capture and ionization (transfer ionization or TI):

$$He^+ + He \text{ -------- } He + He^{2+} + e^- \quad (4)$$

Single ionization of He accompanied by projectile electron loss:

$$He^+ + He \text{ -------- } He^{2+} + He^+ + 2e^- \quad (5)$$

Double ionization of He accompanied by projectile electron loss:

$$He^{+} + He \text{ -------- } He^{2+} + He^{2+} + 3e^{-} \quad (6)$$

A general schematic description of these processes is shown in Figure 1. In our experiment, the projectile (P) is He^{+} and the target (T) is He. When the collision takes place, the projectile may experience no charge change (Figure 1a), it may lose an electron (1b), or it may capture an electron (1c). At the same time, the target may be singly-ionized (solid line only), or doubly-ionized (solid and dashed line).

One of the most useful descriptions of a collision process is the determination of the cross section, in this case, for the various reactions (1) - (6). Typically, such experiments are performed using time-of-flight and coincidence techniques to obtain cross sections for target ionization associated with outgoing projectile ions in a particular charge state. To distinguish the cross sections for different processes, we use the following notations:

$\sigma_{q,q-1}$ ------- total single-electron capture cross section;

$\sigma^{01}_{q,q-1}$ ------- single ionization resulting from one-electron capture by the projectile;

$\sigma^{02}_{q,q-1}$ ------- double ionization associated with one-electron capture by the projectile (transfer ionization);

$\sigma^{01}_{q,q}$ ------- single ionization associated with no projectile charge change;

$\sigma^{02}_{q,q}$ ------- double ionization associated with no projectile charge change;

$\sigma^{01}_{q,q+1}$ ------- single ionization associated with projectile one-electron loss;

$\sigma^{02}_{q,q+1}$ ------- double ionization associated with projectile one-electron loss;

where σ represents the cross section, the superscript gives the initial and final charge states of the target atom, and the subscript gives the initial and final charge states of the projectile ion.

Ion-atom collision interactions can be understood better if cross sections are

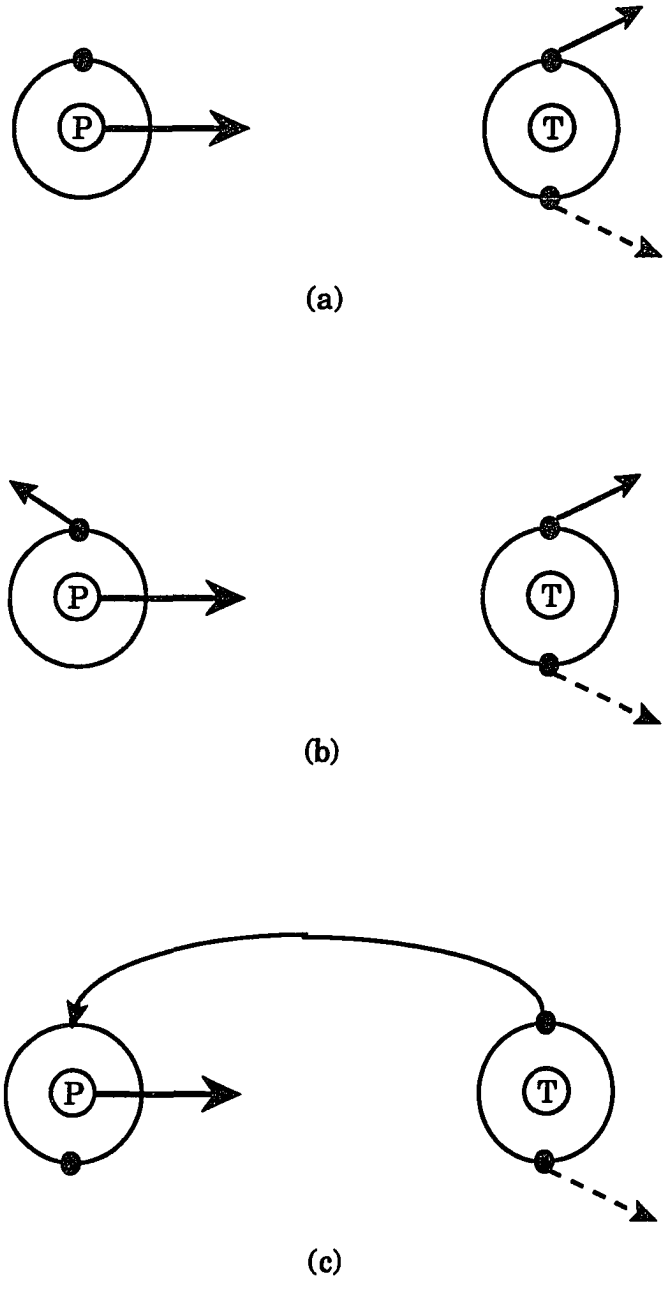

Figure 1. Diagram for Target Single or Double Ionization Associated With No Projectile Charge Change (a), Electron Loss (b), and Electron Capture (c).

available for each given projectile species, charge state, and target over a large energy range. Therefore, there is considerable interest in searching for scaling rules which can help give insight into the dynamics of the collision process. For example, Schlachter et al. (1983) derived a scaling rule for single-electron capture in several targets based on results of electron capture cross sections obtained from a number of different experiments. Later a revised scaling rule (Schlachter et al., 1987) was obtained for a variety of highly charged ions in helium targets:

$$\tilde{\sigma} = 3.52 \times 10^{-9} [1 - \exp(-0.083\, \tilde{E}^{1.33})] \times [1 - \exp(-7.5 \times 10^{-6}\, \tilde{E}^{2.85})] / \tilde{E}^{4.18} \quad (7)$$

with the reduced variables

$$\tilde{\sigma} = \sigma_{q,q-1}\, Z^{1.8} / q^{0.7} \qquad \text{and} \qquad \tilde{E} = E / (Z^{1.25}\, q^{0.5}) \quad (8)$$

At high energies, the cross section approaches:

$$\sigma_{q,q-1} = 3.8 \times 10^{-8}\, q^{2.8} / E^{4.18} \quad (9)$$

where $\sigma_{q,q-1}$ is the cross section (in cm^2) for electron capture, E is the projectile energy in keV/u, q is the projectile charge state, and Z is the target nuclear charge.

Similarly, McKenzie and Olson (1987) obtained a scaling rule for single ionization of He with no projectile charge change (pure single ionization):

$$\sigma_{q,q}^{01} = [(1.46 \times 10^{-17})\, q^{1.78} / (E^{0.78})] \quad (10)$$

where $\sigma_{q,q}^{01}$ is the cross section (in cm^2) for pure single ionization.

Of primary interest in this work is the double ionization of helium. The projectile charge q and impact velocity v are the two important parameters in understanding the interaction mechanisms. The cross sections for single ionization of atoms by fast ions can be well described within the framework of the first Born approximation (Inokuti, 1971; Madison & Merzbacher, 1972), and were found to be proportional to $(q/v)^2(\ln v)$. For double ionization, however, the situation is much more complicated due to electron correlation. It was first proposed by McGuire (1982) that

double ionization by ions at high velocities ($v_{ion} > 10\ v_{Bohr}$) can be understood in terms of two mechanisms: (1) a two-step process (TS), second order in q/v, in which both target electrons are removed in separate direct interactions with the projectile, and (2) a shakeoff process (SO), first order in q/v, in which the first electron is removed in a direct interaction with the projectile while the second electron is ejected when the resulting ion relaxes to a continuum state. The former process is dominant at lower projectile energies, while the latter is dominant at higher projectile energies. A schematic diagram of these mechanisms is shown in Figures 2a and 2b. The two-step process (Figure 2a) involves independent-particle interactions where the projectile interacts with the target electrons separately at different times, whereas the shakeoff process (Figure 2b) is due to electron correlation.

The double ionization process might be more complicated than the model above, however. Andersen et al. (1986) suggested that in an ion-atom collision, an ejected electron may collide with a second electron, resulting in double ionization (Figure 2c). This two-step (second-Born approximation) process was denoted as TS-1, a two-step process involving one interaction with the projectile. The two-step mechanism where both target electrons interact with the projectile separately is then denoted as TS-2. As suggested by McGuire (1984), at high projectile velocities v, the recoil energy of the first target electron is nearly independent of v; therefore TS-1 will probably yield a constant double-to-single ionization ratio in the high energy limit. Thus, the contribution from TS-1 can be included in the SO mechanism, and the TS-1 mechanism will not be considered further here.

The double-ionization cross section σ_{2I} can be expressed as (McGuire, 1982):

$$\sigma_{2I} = |a_{SO}(q/v) + a_{TS}(q/v)^2|^2 \qquad (11a)$$

$$= \sigma_{SO} + \sigma_{int} + \sigma_{TS} \qquad (11b)$$

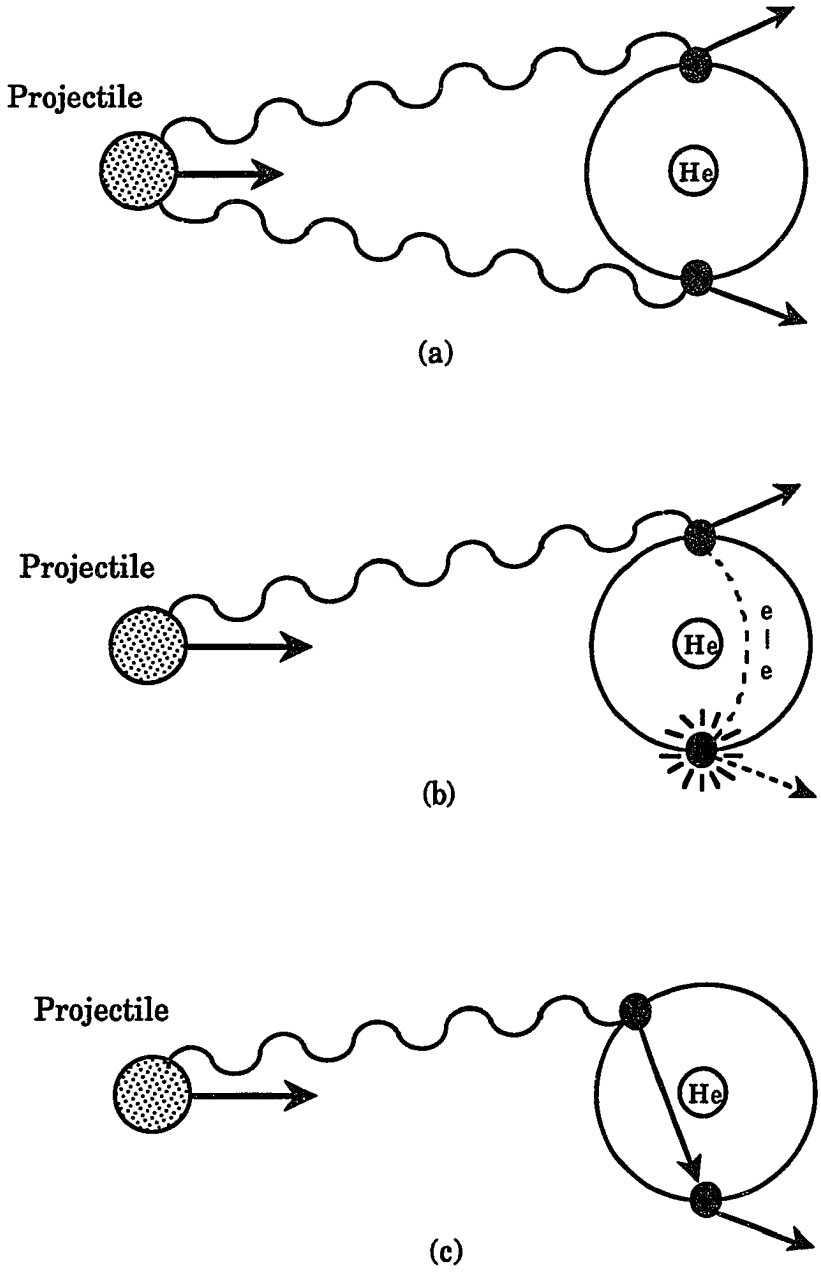

Figure 2. Illustration of Three Mechanisms Leading to the Double Ionization of Helium.

(a) two-step (TS) mechanism (or TS-2 mechanism);
(b) "shakeoff" (SO) mechanism;
(c) TS-1 mechanism.

where the notation SO refers to "shakeoff," TS refers to "two-step," and σ_{int} is the interference cross section resulting from the q^3 cross term.

As the cross section for single ionization by fast ions is accurately known (Inokuti, 1971), it is customary to focus on the ratio of the double-to-single ionization cross sections. This ratio will be expressed as $R = \sigma_{2I} / \sigma_{1I}$, where the subscripts 2I and 1I represent double ionization and single ionization, respectively. To distinguish the ratio for different processes, the following notations will be used:

Ratio of double-to-single ionization associated with projectile one-electron capture:

$$R_{q,q-1} = \sigma^{02}_{q,q-1} / \sigma^{01}_{q,q-1} \tag{12}$$

Ratio of double-to-single ionization associated with no projectile charge change:

$$R_{q,q} = \sigma^{02}_{q,q} / \sigma^{01}_{q,q} \tag{13}$$

Ratio of double-to-single ionization associated with projectile one-electron loss:

$$R_{q,q+1} = \sigma^{02}_{q,q+1} / \sigma^{01}_{q,q+1} \tag{14}$$

Using the first Born approximation, the cross section for single ionization can be expressed as (Inokuti, 1971):

$$\sigma_{1I} = (\text{const}) \times (q/v)^2 \ln v \tag{15}$$

where v is the projectile velocity, and q is the projectile charge.

From Eq. 11, the cross sections for double ionization can be written as follows:

$$\sigma_{SO} = (\text{const}) \times (q/v)^2 \ln v \tag{16}$$

$$\sigma_{int} = (\text{const}) \times (q/v)^3 \tag{17}$$

$$\sigma_{TS} = (\text{const}) \times (q/v)^4 \tag{18}$$

where the (lnv) term in Eq. 16 comes from integration over the tail of the long-range Coulomb potential of the projectile (Inokuti, 1971).

Hence, combining Eqs. (11) and (15)-(18) gives the ratio of double-to-single ionization as follows:

$$R = \sigma_{2I} / \sigma_{1I} = c_{SO} + c_{int} \times \frac{q/v}{\ln v} + c_{TS} \times \frac{(q/v)^2}{\ln v} \qquad (19)$$

where c_{SO} and c_{TS} are constants related to the shakeoff and two-step processes, respectively, and c_{int} is related to the interference between the SO and TS mechanism.

If, however, the interference term is neglected, Knudsen et al. (1984) found an empirical scaling rule for the ratio of double-to-single pure ionization by fitting their experimental results for fully stripped ions to Eq. (19):

$$R_{q,q} = 2.20 \times 10^{-3} + 4.55 \times 10^{-3} \frac{q^2}{E \ln (13.12 \sqrt{E})} \qquad (20)$$

where E is the projectile energy measured in MeV/u.

The first term in Eq. (20) is due to the SO mechanism, while the second term results from the TS mechanism. From Eq. (20), the two-step mechanism is expected to dominate at low projectile energies, while shakeoff is expected to dominate in the limit of high projectile energies. At intermediate energies both the TS and SO mechanisms are expected to contribute significantly to the double ionization of helium. A qualitative description of the ratio R as a function of projectile energy is shown in Figure 3. Presentation of this kind of plot can give us insight into the relative importance of the TS mechanism versus the SO mechanism. As can be seen from the plot, the dashed curve merges into the two-step curve as the projectile energy decreases, and asymptotically goes to a constant value (SO mechanism) as the energy goes higher.

It has been suggested that there is a connection between ionization by charged-particles and by photons (McGuire, 1984). As first suggested by Horsdal-Pedersen and Larsen (1979), the charged-particle high energy limit of double-to-single ionization ratio (R_Z) is expected to be the same as for photoionization (R_γ) if the first electron leaves the target quickly. However, the observed results are not in good agreement with this prediction. The high energy limit for photoionization was found to be about

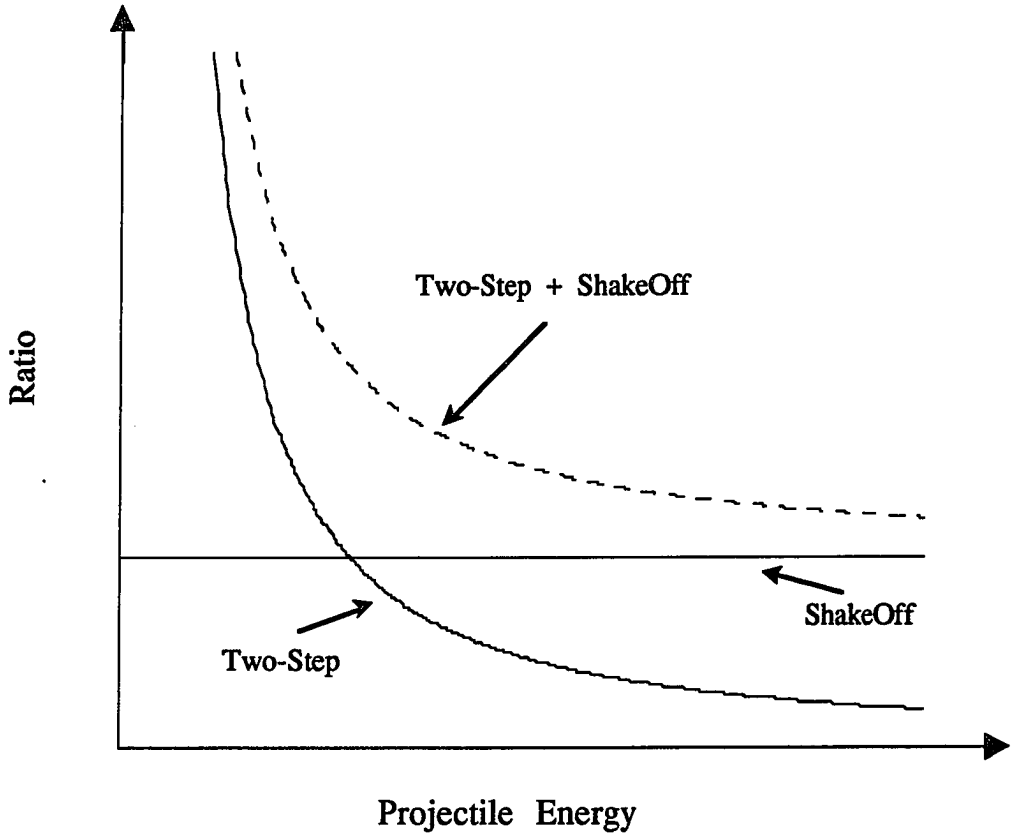

Figure 3. Qualitative Theoretical Prediction of the Ratio of Double-to-Single Ionization Cross Sections as a Function of Projectile Energy.

The solid lines represent double ionization due to two mechanisms: curve: two-step (or independent) mechanism; straight line: shakeoff (or electron correlation) mechanism. The dashed curve is the combination of both mechanisms.

0.034 (Schmidt et al., 1976). For electron and proton impact, however, the high energy limit was about 0.0027 (Haugen et al., 1982; Knudsen et al., 1984), about an order of magnitude smaller than R_γ. Knudsen et al. (1984) obtained an empirical scaling expression for the ratio of double-to-single pure ionization of helium by fully stripped projectiles, and found the high energy limit to be 0.0022, a factor of fifteen smaller than R_γ. McGuire (1984) suggested that this large discrepancy in the high energy limit between photons and charged-particles is mainly due to the fact that the projectile is not annihilated in the case of charged-particles, therefore not all of the collision energy is imparted to the electron, and for charged-particle impact at high velocities most electrons tend to be ejected at moderate velocities which means that correlation between final-state continuum electrons is possible. For double ionization associated with electron capture (TI), however, the first electron leaves with the same speed as that of projectile. Thus, in the high velocity limit for this case, the mechanism for double ionization is expected to be similar to that for photoionization, leading to $R_Z \approx R_\gamma$. Knudsen et al. (1987), however, suggested that the two second Born capture mechanisms (denoted as 2B1 and 2B2) may dominate the TI process at high velocity, and the ratio of double-to-single ionization is expected to be:

$$R_{q,q-1} = \sigma^{02}_{q,q-1} / \sigma^{01}_{q,q-1} = R_\gamma + \left(8\, Z^2 \frac{q + \sqrt{2}\, Z}{q + Z} \right)^{-1} \qquad (21)$$

where Z is the target nuclear charge, and q is the projectile charge state. For He^+ projectiles colliding with He, q=1, Z=2, $R_\gamma = 0.034$, which gives $R_{q,q-1} = 0.058$.

Another interesting behavior of the double ionization process is its projectile charge dependence. As first noticed by Haugen et al. (1982), the double ionization of helium by electrons is a factor of two larger than that for equal velocity proton impact. As single ionization cross sections (which vary as q^2) are well described by the first

Born approximation, and hence give no significant difference between ionization by protons or electrons, it was difficult to understand the difference for double ionization. McGuire (1982) first suggested that the observed difference between protons and electrons was due to a q^3 term resulting from the interference between the TS and SO mechanisms (refer to Eq. 11). Later, an experiment performed by Andersen et al. (1986) using protons and antiprotons showed that for double ionization the antiproton cross sections are about twice as large as those for protons, thereby confirming that the difference between the electron and proton is not due to the large difference in their masses but rather due to their opposite charges.

So far, we have only considered the cases involving fully stripped ions or electrons or photons, in which projectiles were treated as one body or one particle. In the case of partially stripped projectiles with one bound electron orbiting around the nucleus (e.g., He^+, Li^{2+}, Be^{3+}, etc.), the projectiles may not be treatable as one body and the situation becomes much more complicated. As illustrated in Fig. 4a, for fully stripped projectiles which are point-like particles, the double ionization may result either from the Coulomb interaction between the projectile nuclei and the target electrons (n-e) or the interaction between the target electrons (e-e) or both, depending on the impact energy. In the case of He^+ projectiles which carry an electron into the collision (see Fig. 4b), however, double ionization may also result from the Coulomb interaction between the projectile electron and the target electrons, in addition to the two interactions mentioned above. If the electron is weakly bound and the He^+ projectile can be treated simply as one electron and one helium nucleus independent of each other, double ionization cross sections should be the sum of those for He^{2+} ions and those for electrons (two one-body interactions). In reality, however, the Coulomb interaction between the projectile nucleus and its electron (n-e) may not be negligible and should be

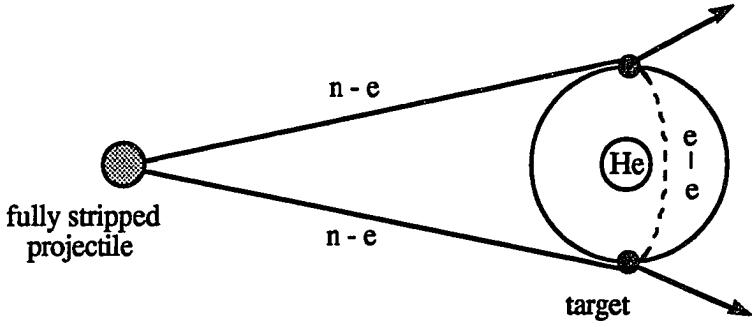

(a)

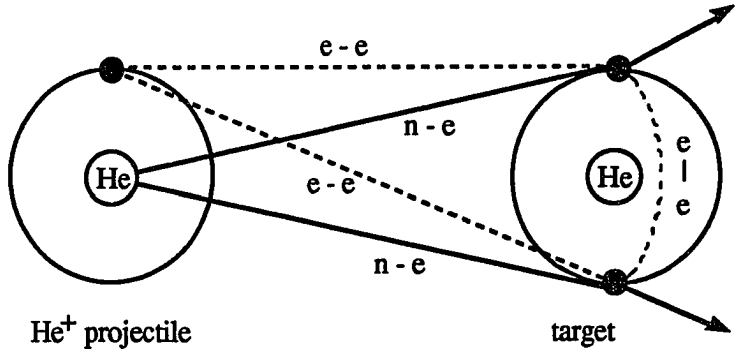

(b)

Figure 4. Illustration of Double Ionization of Helium Caused by Coulomb Interactions Between the Projectile and the Target.

(a). With fully stripped projectiles; (b). with He^+ projectile. The dashed lines labeled e-e represent electron-electron interactions, and the solid lines labeled n-e represent nucleus-electron interactions. The arrows represent ionization of the target electrons.

taken into account. If this n-e interaction is very small compared with the other interactions, it may be treated as a perturbation approximation. If, however, this n-e interaction is comparable to the other interactions, the projectile nucleus and electron should be viewed as two mutually interacting particles (two-body), and the calculations would be much more difficult. The role played by this projectile electron is not accurately known. If, however, the influence on the interaction by this electron is approximated by a screening or antiscreening effect of electron clouds to the projectile nucleus, the interaction picture can be simplified as a point-like projectile interacting with an effective charge $q_{eff}(b)$ which is a function of the impact parameter b (Toburen et al., 1981; McGuire et al., 1981). As suggested by McGuire et al. (1981), for hydrogen-like projectiles (e.g., He^+,Li^{2+}, etc), in the range of the first Born approximation, the projectile may be considered a point particle with an the effective charge q_{eff} expressed as:

$$|q_{eff}(Q)|^2 = Z^2 + 1 - 2Z|1 + (Q/2Z)^2|^{-2} \tag{22}$$

where Z is the projectile nuclear charge, and Q is the momentum transfer.

$$|q_{eff}(Q)|^2 = \begin{cases} (Z-1)^2 & Q \to 0 \ (\text{or } b \to \infty) \\ Z^2 + 1 & Q \to \infty \ (\text{or } b \to 0) \end{cases} \tag{23}$$

where b is the impact parameter. For a bare nucleus, $|q_{eff}(Q)|^2 = Z^2$, which is independent of Q or b.

Consider the He^+ projectile (Z=2). A brief illustration of the scattering mechanism with different impact parameters is shown in Figure 5. At small Q (large impact parameter b), from Eq. (23), $q_{eff} = 1$. The helium projectile nucleus is fully screened by the electron, therefore the He^+ projectile is equivalent to a point-like particle with q=1 (Fig. 5a). At large Q (small b, hard collision), $q_{eff} = \sqrt{5} = 2.24$, and the

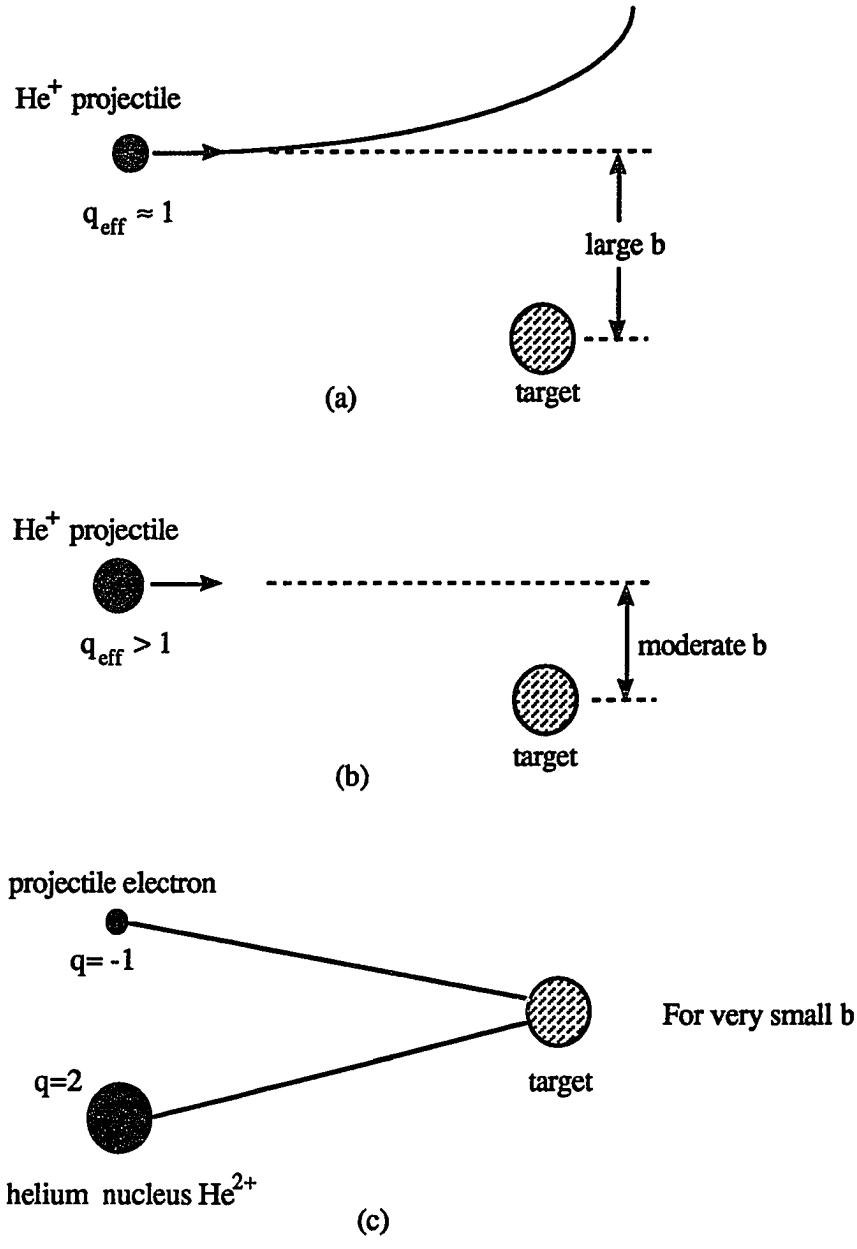

Figure 5. Illustration of Projectile Electron Screening of the Nucleus.

(a) For very large b, the projectile nucleus is fully screened by the electron giving $q_{eff} \approx 1$; (b) for moderate b, the nucleus is partially screened by the electron giving $q_{eff} > 1$; (c) for very small b, the projectile can be viewed as an electron and a nucleus interacting with the target incoherently (free collision model, Bohr, 1948).

projectile nucleus and electron interact with the target incoherently (Fig. 5c). For moderate Q, $1< q_{eff} <2.24$, the magnitude of q_{eff} is dependent on the momentum transfer Q or impact parameter b (Fig. 5b). As suggested by Bohr (1948), the effects of the projectile nucleus and projectile electrons on the target may simply add, therefore the total cross section is a sum of independent cross sections from the bare projectile (He^{2+}) and the electron (free collision model). If the electron and helium nucleus are treated as the same point-like particles with q=1 and 2, respectively, the He^{+} projectile can be viewed as a point-like particle with an effective charge 2.24 (McGuire et al., 1981). However, as mentioned before, the double ionization of helium by electrons is a factor of two larger than that for equal v/q He^{2+} impact due to the interference between TS and SO (McGuire, 1982). Therefore the cross sections for electron impact and He^{2+} impact should be added separately. This was confirmed in an experiment by Wang et al. (1986) using hydrogen atoms colliding with Ar target. Here the cross section for H impact is equal to the sum of cross sections by e^{-} and p^{+} impact.

Using the approximation described above, Wang et al. (1990) predicted that the order of high-energy limits of double-to-single ionization ratios of helium by projectiles with and without electrons is as follows:

$$R_{H+} < R_{H0} < R_{He0} \tag{24}$$

$$R_{H+} = R_{He2+} < R_{He+} < R_{He0} < R_{photon} \tag{25}$$

The model above may be a good qualitative description for projectiles with bound electrons. However, more theoretical studies are necessary to quantitatively describe the various interactions among the many-body particles. Experimentally, the effect caused by the projectile electrons may be extracted from the observed deviation between double ionization by fully stripped ions and by partially stripped ions (He^{+}

here). Since double ionization of helium by fully stripped ions has been widely investigated by various groups (Shah & Gilbody, 1985, H^+, He^{2+}, Li^{3+}; Andersen et al., 1986, p and p^-; Knudsen et al., 1984 and 1987, H^+, He^{2+}; Heber et al., 1990, N^{7+}) and is fairly well understood, the present study of double ionization of helium by He^+ ions can be very useful in understanding the dynamics of ion-atom interactions, and in turn, give us more insight into the many-body problem.

CHAPTER III

EXPERIMENTAL PROCEDURE

The experiment was performed at Western Michigan University (Kalamazoo) using the 6 MV EN tandem Van de Graaff accelerator. A general schematic of the accelerator is shown in Figure 6. Negative helium ions produced from the exchange ion source were accelerated towards the positive terminal of the accelerator, where electrons were stripped off to make the ions positive. The ions were then repelled by the positive terminal, and accelerated a second time. Ions with the desired charge (He^+) were selected by an analyzing magnet and then directed into the atomic physics beam line.

The atomic physics beam line and the target region are shown in Figure 7 and Figure 8, respectively. After passing through two sets of collimating slits, the He^+ beam was directed into the differentially-pumped target gas cell (3.65 cm long) which was bounded by 0.20 cm and 0.31 cm apertures. Two additional apertures (0.20 cm and 0.40 cm in diameter, respectively) located just upstream and downstream from the gas cell provided differential pumping and reduced the scattering of ions from the collimating slits. The gas cell contained ≤ 0.5 mTorr of pure He gas to ensure single collision conditions, and the pressure was measured using a capacitance manometer adjusted with a remotely controlled valve.

After interaction with the target gas, the beam was separated into its various charge-state components (He^0, He^+, He^{2+}) by an analyzing magnet. As seen from Fig. 7, ions having the same outgoing charge state as the incident projectile ions, He^+ (or Q), were collected in a Faraday cup, while the ions that captured an electron, He^0 (or

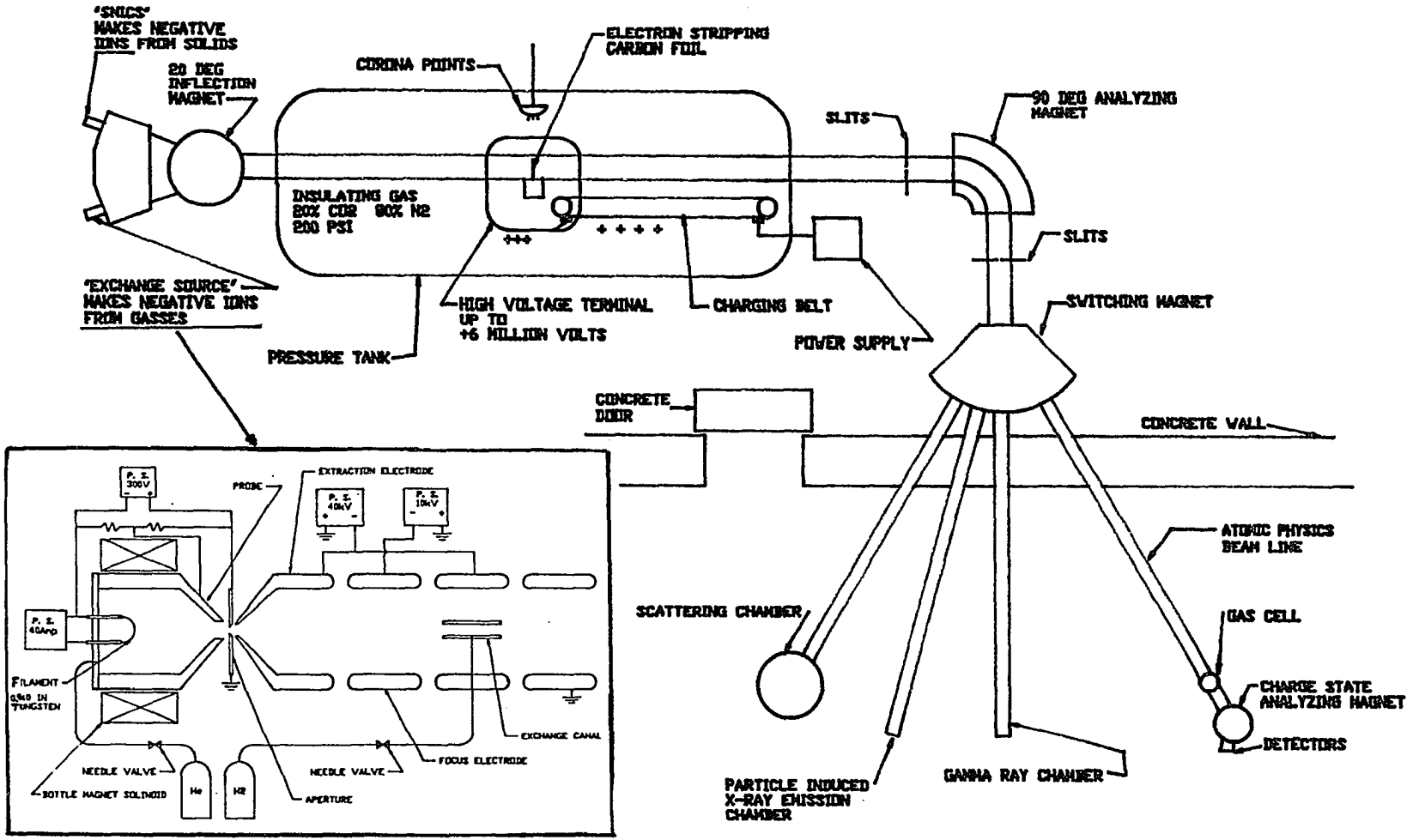

Figure 6. General Schematic of the WMU 6MV EN Tandem Van de Graaff Accelerator.

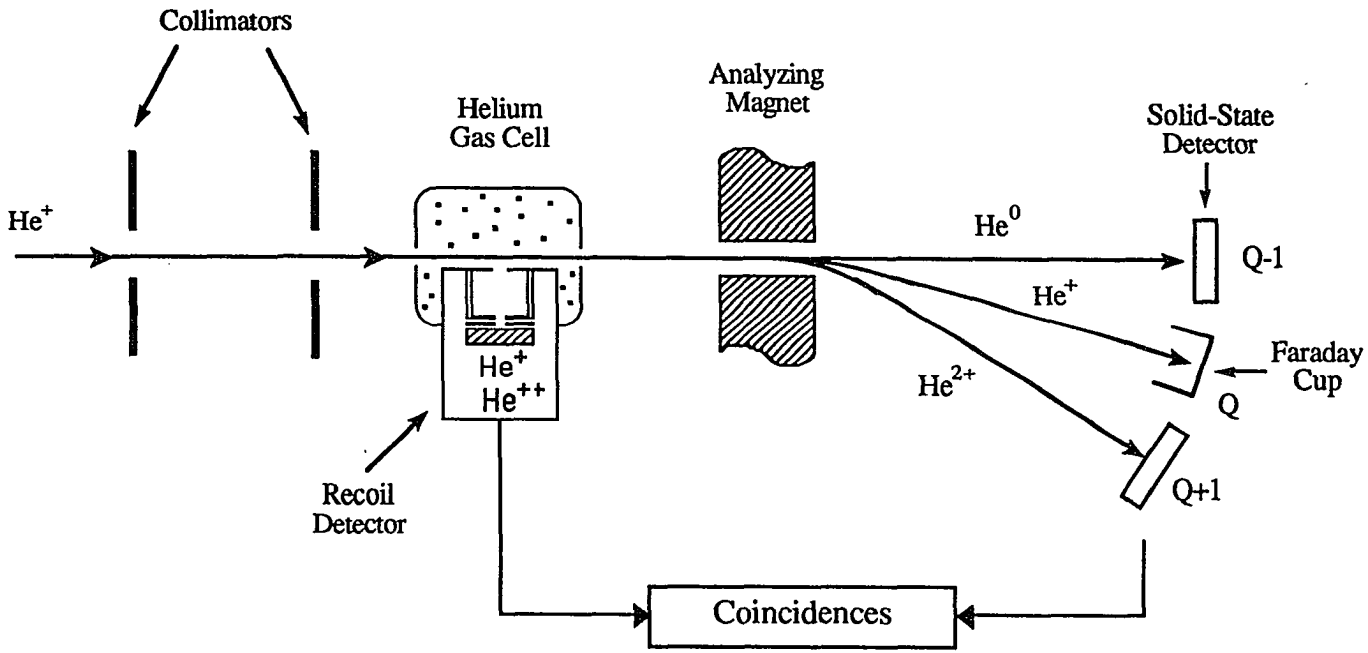

Figure 7. Schematic of the Atomic Physics Beam Line at WMU.

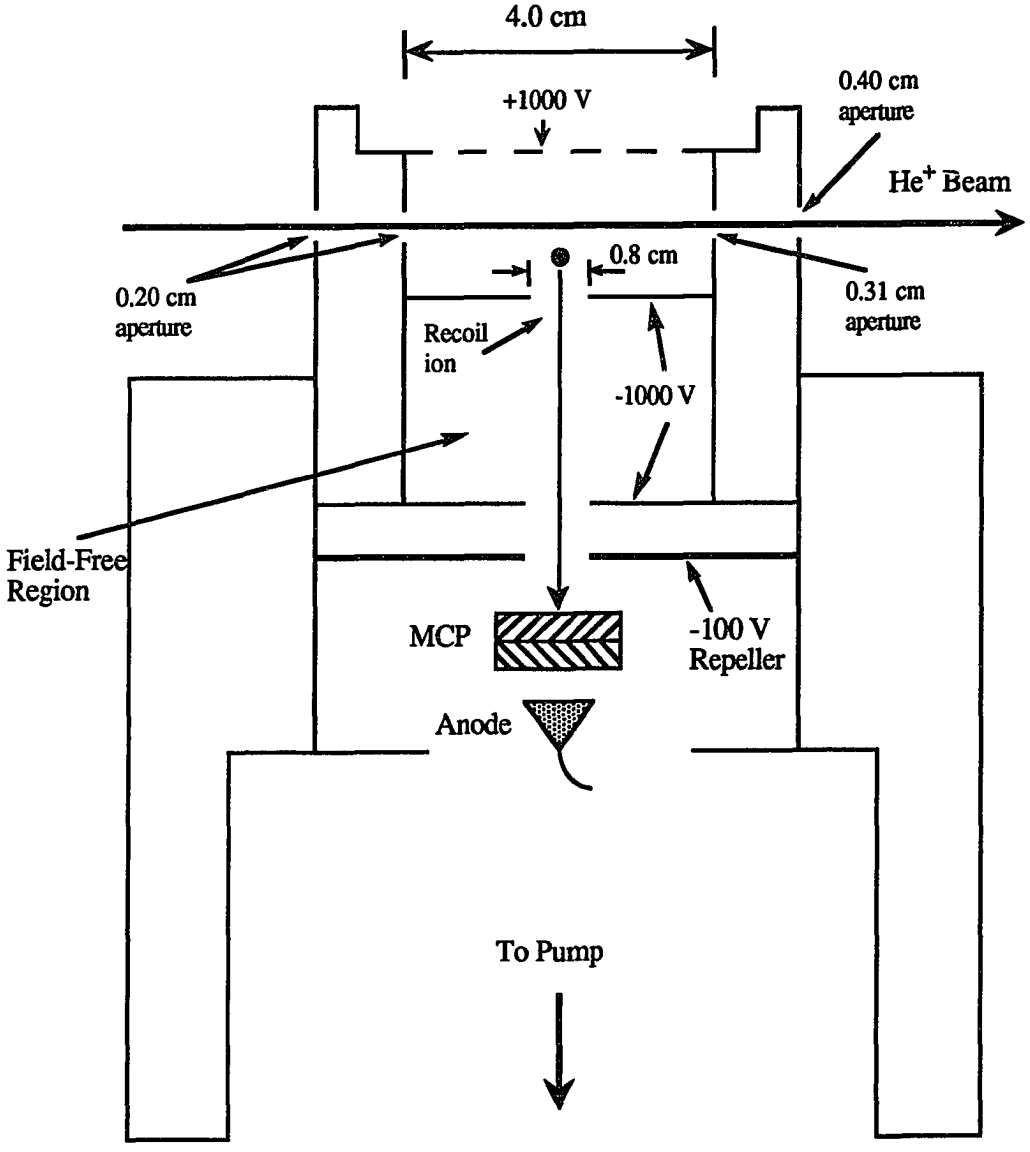

Figure 8. Schematic of the Target Region Consisting of a Differentially Pumped Gas Cell and Time-of-Flight Recoil-Ion Detector.

Q-1), or lost an electron, He^{2+} (or Q+1), were detected with solid-state detectors. The charge-changed particles striking each of the solid-state detectors were counted with a scaler, while the main beam component (Q) was measured with a Keithley electrometer, and then digitized with a current integrator so that the total number of incident ions could be determined for each measurement.

The recoil detector system (Figure 8) was designed such that recoil ions of a specific charge state have approximately the same flight time, regardless of the exact location of their creation in the interaction region, whereas ions of different charge state will have different flight times (time-of-flight technique). This technique allows the helium recoil ions (He^+ and He^{++}) to be distinguished and measured separately. As shown in Figure 8, the slow He^+ and He^{++} recoiling ions were extracted and accelerated perpendicular to the beam direction towards the 0.8-cm aperture by two electrodes, held at +1000 and -1000 volts. After drifting through a field-free region, the recoil ions passed through a repelling grid, held at -100 volts (to suppress electrons), and then were detected by a negatively biased microchannel plate (MCP). The MCP anode provided an output signal for timing and counting purposes.

With the recoil ions generating the start pulses and the projectile signals from the solid-state detectors generating the stop pulses, a standard coincidence technique was used to detect coincidences between the occurrence of singly- or doubly-charged helium recoil ions and outgoing projectile ions capturing or losing an electron. A block diagram of the electronics system is shown in Figure 9. Signals from the microchannel plate (MCP) were passed through a fast timing amplifier (FTA) and a timing filter amplifier (TFA), and then routed to a constant fraction discriminator (CFD) which converted the analog signal to a logic signal. The output of CFD was then routed through a fan in/fan out which produced two isolated signals, one of which was used

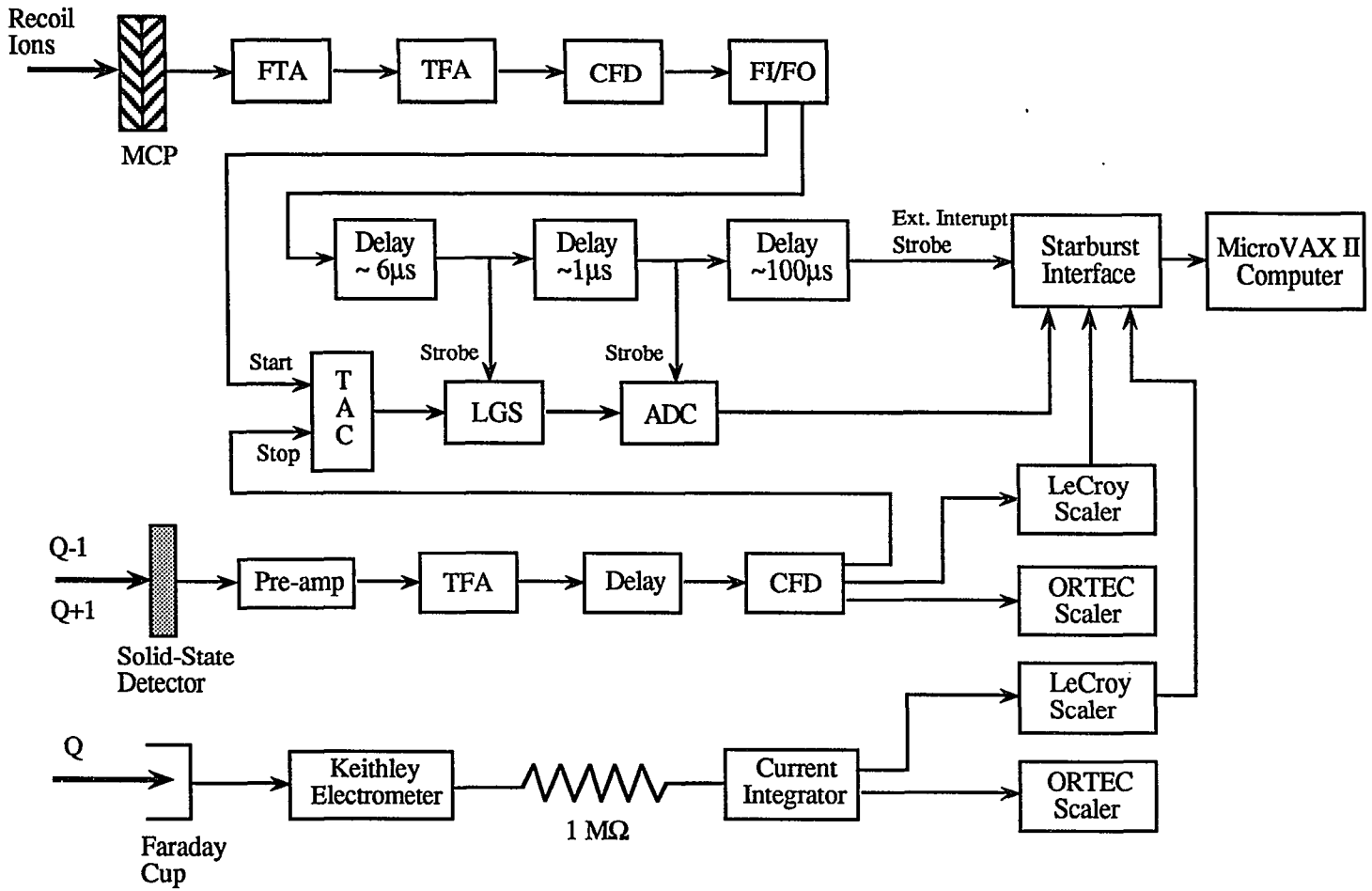

Figure 9. Block Diagram of the Electronics Used for Detecting Charge-Changed Projectile Ions in Coincidence With Target Recoil Ions.

as a START for a time-to-amplitude converter (TAC). Since the electronics are identical for the Q-1 and Q+1 signal channels resulting from charge-changed helium ions striking the solid-state detectors, only one of these channels is shown in Figure 9. The output signal from the solid-state detector was routed through a preamplifier and a timing filter amplifier (TFA), and was then delayed by 100-300 ns (using long cables) before reaching the constant fraction discriminator. One of the outputs from the CFD was used as a STOP for the time-to-amplitude converter (TAC). The TAC outputs a signal whenever a START and a STOP are received within the full-scale time range selected on the TAC. The amplitude of this signal is proportional to the time difference between the START and the STOP signals, and was used to determine the charge state of the recoiling helium ion. The signal from the TAC was conditioned by a linear-gate-stretcher (LGS) before being analyzed by an analog-to-digital converter (ADC). The digital output from the ADC was then input to a Starburst interface prior to transfer to a MicroVAX II computer system for "sorting" and storage.

The main beam current (typically <20 pA) was measured with a Keithley electrometer. The incident particle yield was then obtained by integrating the current over the time required for the measurement using a beam current integrator (BCI). One output from the BCI entered the LeCroy scaler, while another output entered the ORTEC scaler. Both scalers were used to independently give the total number of incident particles.

CHAPTER IV

DATA ANALYSIS

Measurements were carried out with projectile energies 0.125, 0.15, 0.2, 0.25, 0.5, 1, 1.5, 2, 2.5, and 3 MeV/u for the He^+ beam, and 0.5, 1, 1.5 MeV/u for the He^{2+} beam. For each particular projectile energy, measurements were taken at different target gas cell pressures (typically at 0, 0.3, and 0.5 mTorr). Representative coincidence spectra resulting from a run at a given pressure are shown in Figure 10. The spectrum for each run was analyzed to obtain the fractional yield (number of coincidences detected divided by the total number of incident particles) which was then plotted as a function of the gas cell pressure (Figure 11). A linear least-squares fit to the plotted data was used to obtain the slope which, in turn, is related to the cross section. Most of the plots exhibited a linear relationship between the fractional yield and pressure indicating that single collision conditions prevailed within the target region (see Figure 11). A few plots, however, showed nonlinearity between fraction and pressure which indicated that double collisions might have occurred and thus not all of the coincidence events recorded represent valid events. If double collisions did happen, corrections to the cross sections have to be made. This will be discussed at the end of this chapter.

The raw data are simply the numbers of counts obtained from each particle detector or the number of coincidence events recorded for He^+ and He^{++}. The total numbers of incident particles were obtained from the LeCroy scalers or ORTEC scalers, while the number of coincidence events were obtained from spectra such as those shown in Fig. 10. To obtain cross section values, the data were analyzed as

described immediately below.

Let N_{q-1}, N_q, N_{q+1} be the numbers of projectile ions which undergo electron capture, no charge change and electron loss, respectively (single events). Let N_c be the number of coincidence events. Then the total number of incident particles I_0 is given by:

$$I_0 = N_{q-1} + N_q + N_{q+1} \tag{26}$$

In this work N_q was calculated from the current integration (see Fig. 9) as follows (Boman, 1988):

$$N_q = \frac{\text{scaler counts}}{q \times 1.6 \times 10^{-19}} \times \frac{(\text{Keithley scale}) \times (1 \times 10^{-8})}{\frac{2\ V}{1 \times 10^6\ \Omega}} \tag{27a}$$

$$= \frac{(\text{conversion factor}) \times (\text{scaler counts}) \times (\text{Keithley scale})}{q} \tag{27b}$$

where the conversion factor = $3.125 \times 10^{16}\ A^{-1}$. In most cases, the Keithley scale was set to 2×10^{-11} A. Therefore,

$$N_q = \text{scaler counts} \times 6.25 \times 10^5 / q \tag{28}$$

The fractional yield is defined as:

$$F = \frac{\text{number of particles detected for a given process}}{\text{total number of incident particles}}$$

$$= N / I_0 \qquad (N \text{ represents } N_{q-1},\ N_{q+1}, \text{ or } N_c) \tag{29}$$

For each projectile energy, fractions were calculated and plotted versus the gas pressure P. As mentioned earlier, in most cases the fractions were linear with the pressure. A linear least-squares fit was applied to the data to get the slopes of the lines which were then used to obtain cross section values as described below.

The number of detected particles following passage through the target region is

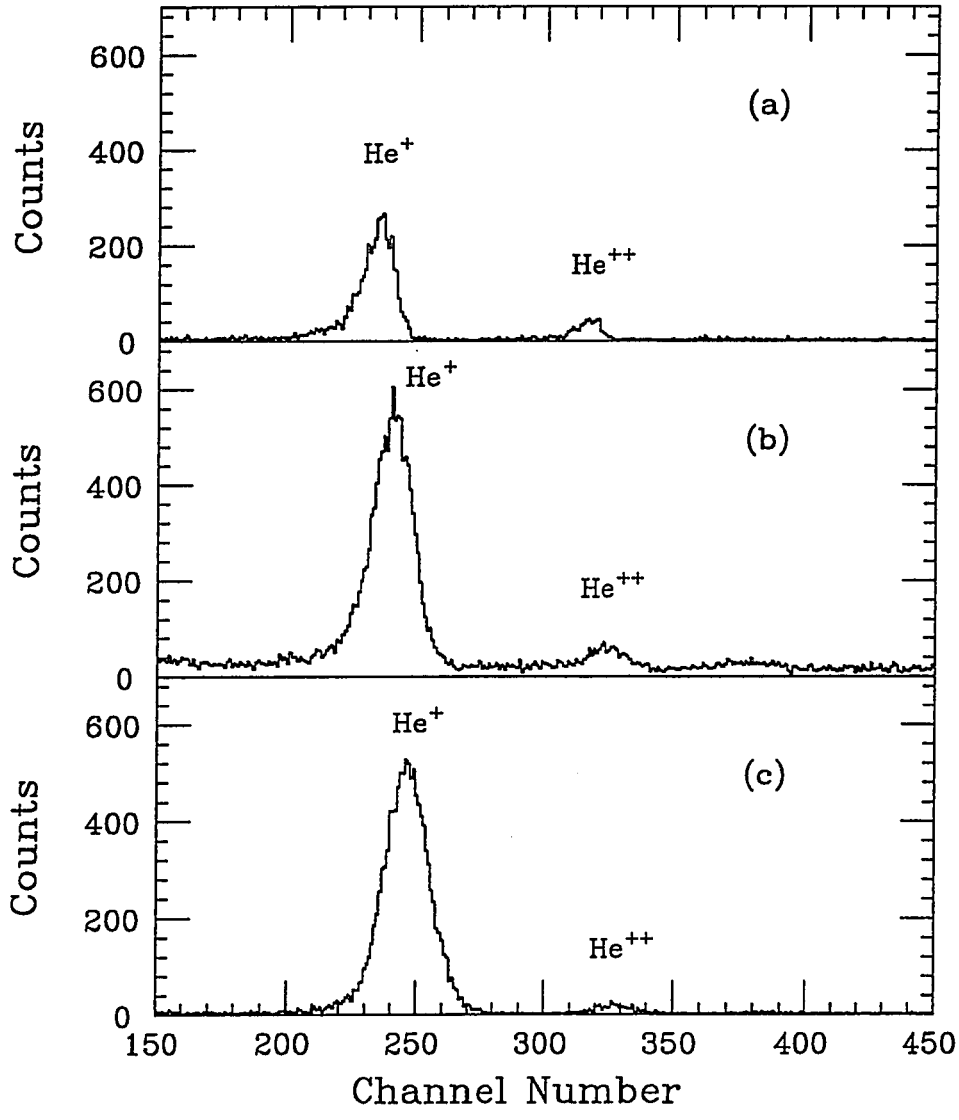

Figure 10. Typical Spectra for Single and Double Ionization of Helium in Coincidence With Projectile (a) Electron Capture; (b) Electron Loss; (c) No Charge Change.

The projectile energy is 0.25 MeV/u, and the gas pressure is 0.5 mTorr.

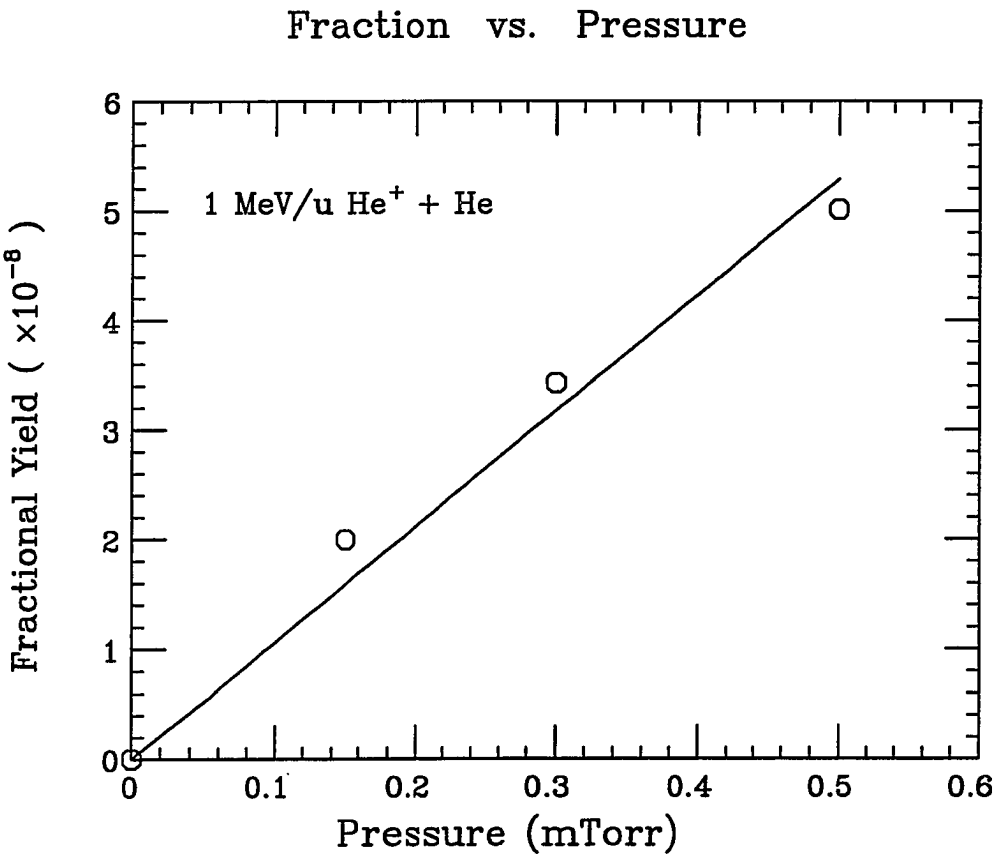

Figure 11. Typical Fractional Yield for Target Single Ionization Coincident With Single-Electron Capture as a Function of Gas Pressure.

given by:

$$N = I_0 \sigma T \varepsilon \tag{30}$$

where I_0 is the number of incident particles in atoms, σ is the cross section in cm^2, T is the target thickness in atoms/cm^2, and ε is the detection efficiency. The target thickness T can be expressed as:

$$T = N_0 P L \tag{31}$$

where $N_0 = 3.3 \times 10^{13}$ atoms / mTorr cm^3, P is the gas pressure in mTorr, and L is the target length in cm. Combining Eqs. (29), (30) and (31) gives:

$$N = I_0 \sigma P N_0 L \varepsilon \tag{32}$$

$$F = \sigma P N_0 L \varepsilon \tag{33}$$

$$\Delta F = \sigma N_0 L \Delta P \varepsilon \tag{34}$$

Therefore, the cross section is given by:

$$\sigma = \frac{(\Delta F/\Delta P)}{N_0 L} \times \frac{1}{\varepsilon} \tag{35}$$

where $\Delta F/\Delta P$ represents the slope of the fraction vs. pressure plot (Fig. 11) which can be obtained directly from the linear least-squares fit.

For the singles measurements (total projectile electron capture or loss) and the coincidence measurements (target ionization associated with projectile electron capture, loss, or no charge change), the values of L and ε are different. The physical length of the gas cell is 3.65 cm, while the recoil detector aperture is only 0.8 cm. Furthermore, the particle detectors are 100% efficient, while the recoil detector is not.

Additionally, for the singles cross sections, the length of the gas cell has to be corrected (Ramsey, 1956; Borman, 1988) due to pressure variations near the entrance and exit apertures:

$$L_{eff} = L + (C1 + C2)/\sqrt{2} \tag{36}$$

where L_{eff} is the effective gas cell length, and C1, C2 are the diameters of the two apertures. In the present experiment, L = 3.65 cm, C1 = 0.20 cm, C2 = 0.31 cm, giving L_{eff} 4.0 cm. Thus, the recoil detector aperture (0.8 cm) is only one fifth of the effective gas cell length.

Then the cross sections for the singles and coincidence measurements can be expressed as follows:

$$\sigma = \frac{(\Delta F/\Delta P)}{N_0 L_{eff}} \qquad \text{for singles} \qquad (37)$$

$$\sigma = \frac{(\Delta F/\Delta P)}{N_0 (L_{eff}/5)} \times \frac{1}{\varepsilon} \qquad \text{for coincidence} \qquad (38)$$

Since the sum of the cross sections for electron capture in coincidence with single and double ionization of helium must be equal to the total cross section for projectile single-electron capture, i.e.,

$$\sigma_{q,q-1} = \sigma^{01}_{q,q-1} + \sigma^{02}_{q,q-1} \qquad (39)$$

the efficiency ε can be obtained from the ratio of the sum of the measured coincidence cross sections for capture to the total capture cross sections:

$$\varepsilon = (\sigma^{01}_{q,q-1} + \sigma^{02}_{q,q-1}) / \sigma_{q,q-1} \qquad (40)$$

From previous experiments (Tanis et al., 1991), ε was found to be 60% for our recoil detector.

As mentioned before, if double collisions did occur, corrections to the cross sections have to be made. To calculate the probability of the occurrence of a double collision, consider the cross section for target single-ionization resulting from projectile electron capture, i.e., $\sigma^{01}_{q,q-1}$. In the present work, the gas cell length is 4 cm, and the detection region (region II) is 0.8 cm, located at the center of the gas cell (see the sketch on the next page). If a double collision occurs in the gas cell, then there are two possible processes which can contribute to an invalid coincidence event: (1) the

projectile first collides with a helium atom in region I, captures an electron, then enters the detection region (region II). This projectile with one electron captured then collides with a second helium atom and results in target single-ionization in the detection region. The TAC will receive signals from the recoil detector and solid-state detector, and an invalid single capture coincidence event is recorded. (2) the projectile collides with a helium atom in the detection region and singly ionizes the atom. This projectile with the same charge state enters region III and collides with a second helium atom and captures an electron from the atom. Again, an invalid single capture coincidence event is recorded.

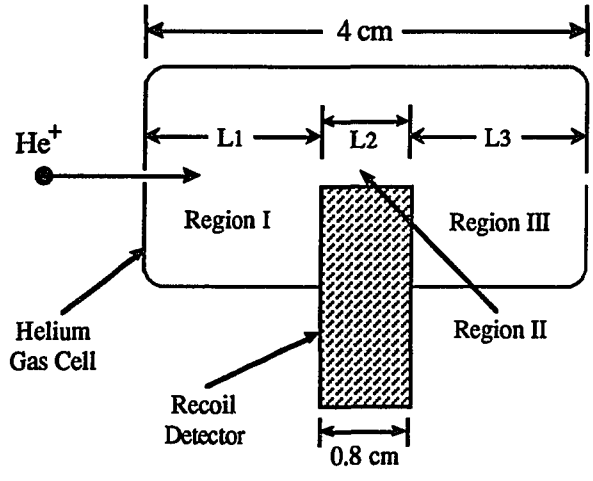

Therefore, the total single capture coincidence events recorded are given by:

$$N^{01}_{q,q-1} = I_0 [(\sigma_{q,q-1} T_1)(\sigma^{01}_{q-1,q-1} T_2) + (\sigma^{01}_{q,q-1} T_2) + (\sigma^{01}_{q,q} T_2)(\sigma_{q,q-1} T_3)] \quad (41)$$

where T_1, T_2, and T_3 are the lengths of region I, region II, and region III in (atom/cm^2), respectively. From Eq. (31), we have:

$$T_i = N_0 P L_i \qquad i = 1, 2, 3 \quad (42)$$

where L_i (i = 1, 2, 3) are the physical lengths of region I, region II and region III. From the sketch, $L_2 = 0.8$ cm, $L_1 = L_3 = 1.6$ cm.

The first and third terms in Eq. (41) are due to double collisions, while the second term represents the coincidence events of interest. By substituting the necessary values into Eq. (41), the contributions from double collisions and single collisions can be calculated. It is found that the contribution from double collisions is less than 1% of that from the single collisions. Calculations were also carried out for all other coincidence processes, and single collision contributions were found to prevail in all cases, therefore no corrections to the cross sections were necessary.

Errors in the cross sections obtained are due to gas pressure uncertainties (3%), fluctuations in the beam current (3%), effective length of the gas cell (<7%), efficiency of the recoil detector (10%), and the least-squares fit to the fraction vs. pressure data (typically <10%), giving an overall absolute uncertainty in the measured coincidence cross sections of ±16%.

CHAPTER V

RESULTS AND DISCUSSION

The cross sections for projectile single-electron capture and loss, along with the relative uncertainties, are listed in Table 1. The notation is described in Chapter II. The numbers in brackets represent powers of ten. These cross sections for He^+ ions, together with the scaling of Schlachter et al. (1987) for electron capture, and the Chebyshev fit for electron capture and loss from the compilation of Barnett et al. (1990) are plotted as a function of energy in Figure 12. As can be seen, the present cross sections for electron capture decrease with energy from 10^{-17} to 10^{-21}, while the present cross sections for electron loss are less energy dependent, and are generally much larger than those for electron capture. Compared to the results from Schlachter et al. (1987) for q=1 projectiles and from Barnett et al. (1990), the present results are in reasonably good agreement at lower energies, but deviate somewhat at higher energies.

The coincidence cross sections for target single and double ionization associated with projectile electron capture, electron loss, and no charge change are given in Tables 2-4, and are plotted in Figure 13. Over most of the energy range investigated, the measured cross sections decrease with energy. Cross sections for single ionization are in all cases larger than those for double ionization. Cross sections for pure single ionization (no projectile charge change) by both He^+ and He^{2+} projectiles are compared with the calculations of McKenzie and Olson (see Eq. 10), and with results from Wood et al. (1986) and Shah and Gilbody (1985) in Figure 14. The results from the several different groups basically agree with each other, and follow the trend predicted by the scaling of McKenzie and Olson (1987). The present data for He^+ and He^{2+} projectiles

Table 1

Cross Sections for Single-Electron Capture and Loss
of He^+ Projectile Ions Colliding
With Helium Target Atoms

E (MeV/u)	$\sigma_{q,q-1}$ (cm^2)	$\sigma_{q,q+1}$ (cm^2)
0.125	(2.30 ± 0.05) [-17]	(2.14 ± 0.11) [-17]
0.150	(1.44 ± 0.02) [-17]	(2.38 ± 0.13) [-17]
0.200	(7.16 ± 0.02) [-18]	(2.77 ± 0.10) [-17]
0.250	(3.86 ± 0.09) [-18]	(2.63 ± 0.08) [-17]
0.500	(3.64 ± 0.02) [-19]	(1.92 ± 0.05) [-17]
1.000	(3.14 ± 0.20) [-20]	(1.42 ± 0.05) [-17]
1.500	(7.52 ± 0.47) [-21]	(8.26 ± 0.76) [-18]
2.000	(3.14 ± 0.15) [-21]	(5.96 ± 0.75) [-18]
2.500	(1.90 ± 0.02) [-21]	(6.14 ± 1.61) [-18]
3.000	(1.14 ± 0.08) [-21]	(8.56 ± 0.38) [-18]

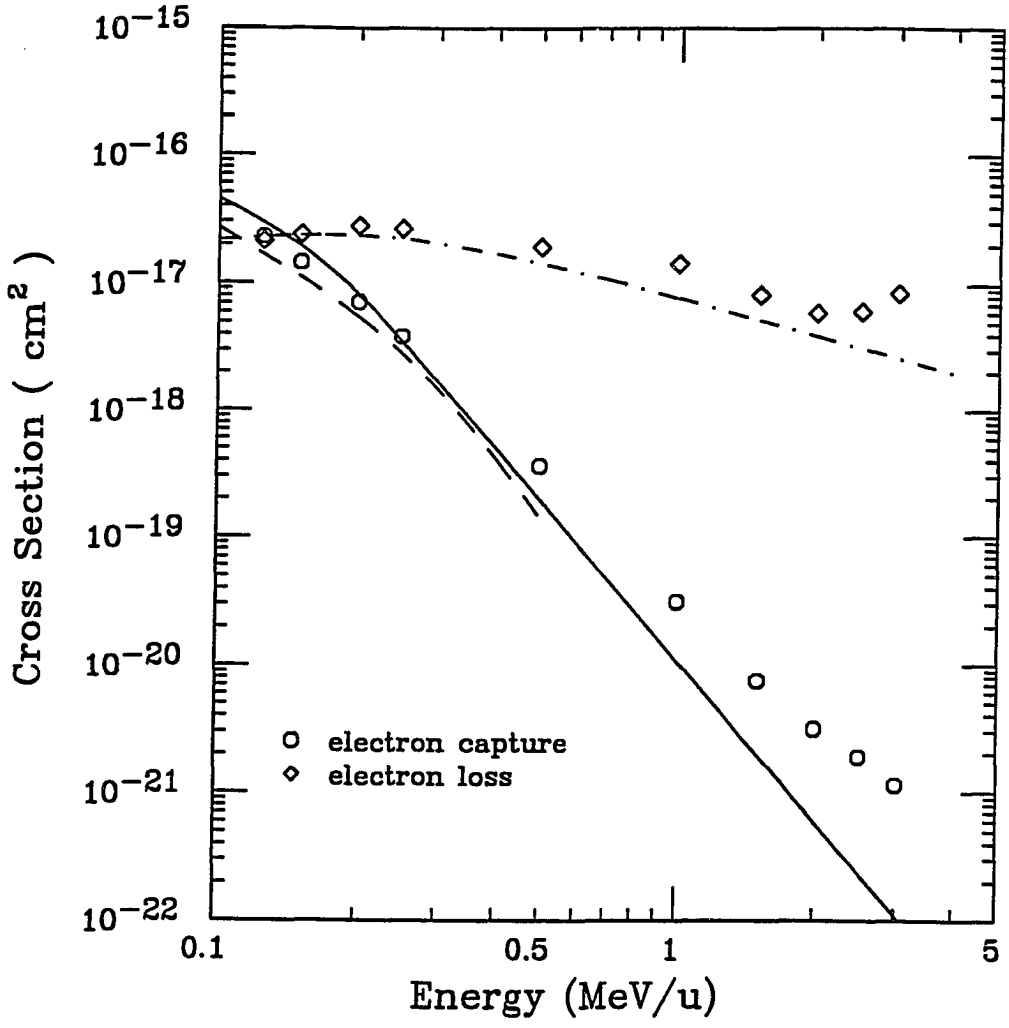

Figure 12. Cross Sections for Projectile Single-Electron Capture and Loss as a Function of Incident Projectile Energy.

The data points are the present results. The dashed and dot-dashed lines are the Chebyshev fits from the compilation of Barnett et al. (1990) for electron capture and electron loss, respectively. The solid line represents the scaling of Schlachter et al. (1987) for electron capture for q=1 projectiles.

Table 2

Cross Sections for Single and Double Ionization of Helium Coincident With Projectile Electron Capture

E (MeV/u)	$\sigma^{01}_{q,q-1}$ (cm^2)	$\sigma^{02}_{q,q-1}$ (cm^2)
0.125	(5.73 ± 0.21) [-18]	(9.72 ± 0.51) [-19]
0.150	(3.47 ± 0.52) [-18]	(5.93 ± 1.01) [-19]
0.200	(9.66 ± 1.83) [-19]	(1.62 ± 0.28) [-19]
0.250	(5.28 ± 0.78) [-19]	(6.94 ± 0.88) [-20]
0.500	(8.59 ± 1.33) [-20]	(9.09 ± 0.95) [-21]
1.000	(6.69 ± 0.32) [-21]	(5.28 ± 0.25) [-22]
1.500	(1.00 ± 0.09) [-21]	(6.69 ± 1.01) [-23]
2.000	(3.59 ± 0.42) [-22]	

Table 3

Cross Sections for Single and Double Ionization of Helium Coincident With Projectile Electron Loss

E (MeV/u)	$\sigma^{01}_{q,q+1}$ (cm^2)	$\sigma^{02}_{q,q+1}$ (cm^2)
0.125	(2.35 ± 0.02) [-18]	(1.27 ± 0.05) [-19]
0.150	(2.80 ± 0.43) [-18]	(2.18 ± 0.27) [-19]
0.200	(1.56 ± 0.31) [-18]	(1.16 ± 0.23) [-19]
0.250	(1.45 ± 0.26) [-18]	(1.04 ± 0.13) [-19]
0.500	(1.59 ± 0.32) [-18]	(7.20 ± 1.52) [-20]
1.000	(1.26 ± 0.08) [-18]	(3.62 ± 0.32) [-20]
1.500	(9.09 ± 0.63) [-19]	(2.21 ± 0.16) [-20]
2.000	(7.89 ± 0.44) [-19]	(1.84 ± 0.12) [-20]
2.500	(6.94 ± 0.13) [-19]	(1.41 ± 0.03) [-20]
3.000	(6.12 ± 0.03) [-19]	(1.02 ± 0.04) [-20]

Table 4

Cross Sections for Single and Double Ionization
of Helium Coincident With Projectile
No Charge Change

E (MeV/u)	$\sigma^{01}_{q,q}$ (cm^2)	$\sigma^{02}_{q,q}$ (cm^2)
	He^+ Projectile	
0.125	(5.33 ± 0.09) [-17]	(2.14 ± 0.11) [-18]
0.150	(7.60 ± 0.03) [-17]	(3.02 ± 0.05) [-18]
0.200	(6.28 ± 0.04) [-17]	(1.94 ± 0.02) [-18]
0.250	(4.67 ± 0.03) [-17]	(1.44 ± 0.10) [-18]
0.500	(2.95 ± 0.08) [-17]	(5.64 ± 0.19) [-19]
1.000	(1.72 ± 0.06) [-17]	(3.08 ± 0.18) [-19]
1.500	(1.18 ± 0.01) [-17]	(1.12 ± 0.06) [-19]
2.000	(9.73 ± 0.52) [-18]	(8.00 ± 0.35) [-20]
2.500	(8.51 ± 0.17) [-18]	(5.66 ± 0.24) [-20]
3.000	(7.01 ± 0.06) [-18]	(4.77 ± 0.34) [-20]
	He^{2+} Projectile	
0.500	(8.33 ± 0.15) [-18]	(1.74 ± 0.11) [-19]
1.000	(6.37 ± 0.13) [-18]	(6.84 ± 0.25) [-20]
1.500	(4.67 ± 0.05) [-18]	(3.53 ± 0.42) [-20]

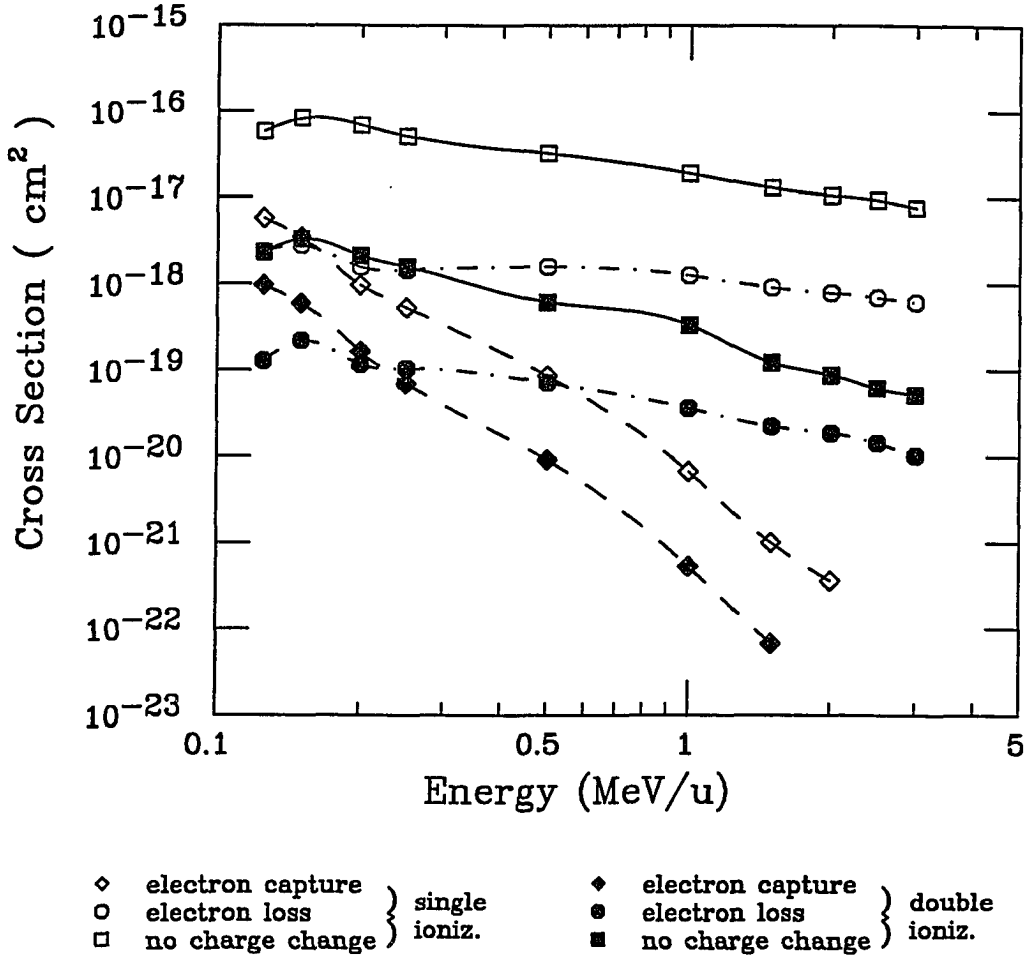

Figure 13. Cross Sections for Single and Double Ionization of Helium by He^+ Ions Undergoing Electron Capture, Electron Loss, and No Charge Change.

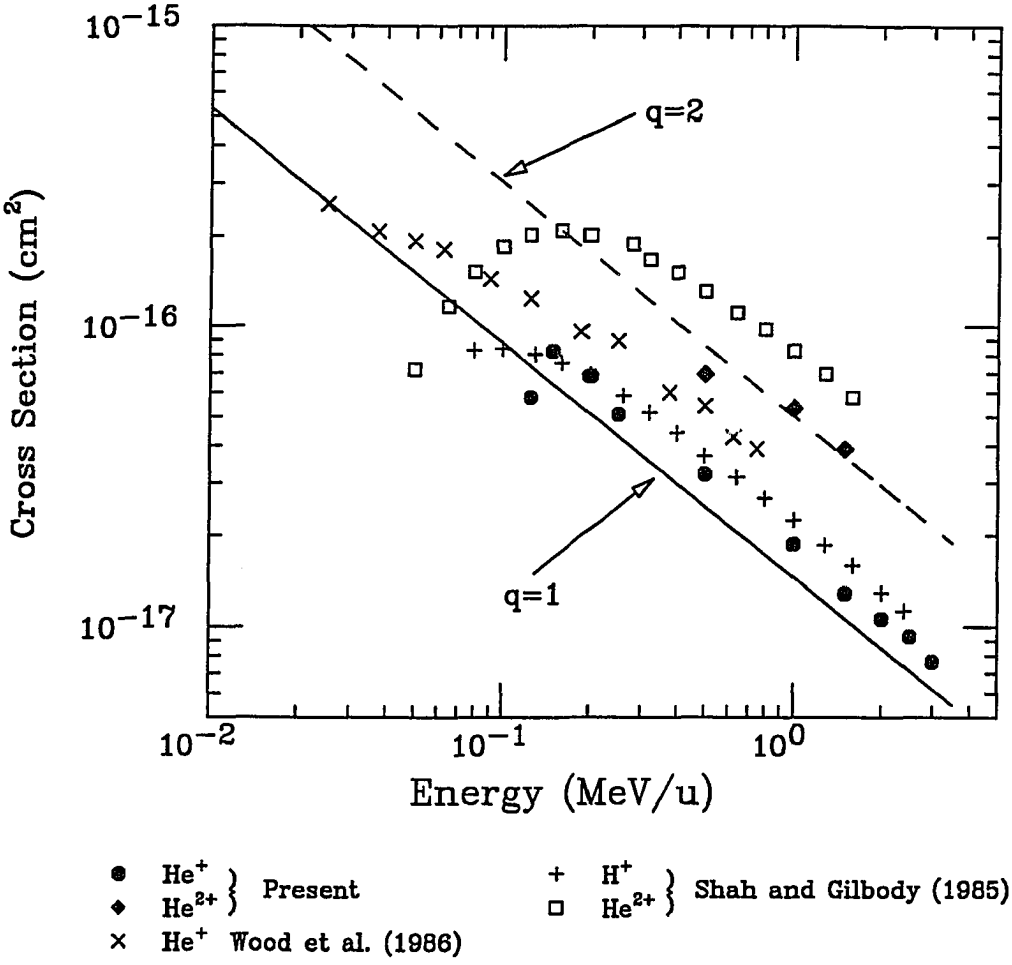

Figure 14. Comparison of the Cross Sections for Pure Single Ionization by He^+ and He^{2+} Projectiles With the Scaling of McKenzie and Olson, and With Results From Wood et al., and Shah and Gilbody.

The solid and dashed curves represent the scaling for q=1 and q=2 projectiles, respectively.

are in reasonably good agreement with the calculation except 10% larger for He^+ projectiles.

As mentioned before, the ratio of double-to-single ionization is an important parameter in understanding the two-step and shakeoff mechanisms in the double ionization of helium. The ratio can be obtained either directly from the spectra (Fig. 10) or from the cross sections. The present results obtained by both methods show good agreement, and therefore, only ratios obtained from the cross sections are shown in Table 5. These data, together with the empirical prediction of Knudsen et al. (1984) for fully stripped projectiles (see Eq. 20) and the pure ionization results for He^+ projectiles from Wood et al. (1986), are shown in Figure 15. In general, the ratios decrease with projectile energy (for energies greater than about 0.1 MeV/u), and they all follow the trend expected from the combination of the two-step and shakeoff mechanisms (refer to Figure 3). The ratio associated with electron capture is larger than that associated with electron loss, and both are larger than that associated with no projectile charge change. A possible explanation for the large R values is that target ionization associated with projectile capture or loss should occur at smaller average impact parameters than that for pure target ionization, thereby leading to a higher probability for double ionization in the former cases. Over the projectile energy range investigated, the present ratio for pure ionization is in reasonable agreement with the results from Wood et al. (1986). Both of these results, however, deviate somewhat from the empirical scaling of Knudsen et al. (1984) (for q=1 projectiles), however.

Of primary interest in this work is the high energy limit of the ratio. As suggested by Knudsen et al. (1984), this ratio should be proportional to $q^2/(E\ln(13.12\sqrt{E}))$ (refer to Eq. 20). Hence, the ratios are plotted as a function of this scaled energy for the full energy range investigated (Figure 16a) and in the high energy

Table 5

Ratios of Double-to-Single Ionization of Helium in Coincidence With Projectile Electron Capture, Electron Loss and No Charge Change

E (MeV/u)	$R_{q,q-1}$ ($\times 10^{-1}$)	$R_{q,q+1}$ ($\times 10^{-2}$)	$R_{q,q}$ ($\times 10^{-2}$)
		He^+ Projectile	
0.125	1.70 ± 0.11	5.39 ± 0.22	4.01 ± 0.22
0.150	1.71 ± 0.39	7.79 ± 1.54	3.98 ± 0.06
0.200	1.68 ± 0.43	7.45 ± 2.08	3.09 ± 0.04
0.250	1.31 ± 0.26	7.16 ± 1.58	3.09 ± 0.22
0.500	1.06 ± 0.20	4.52 ± 1.32	1.91 ± 0.08
1.000	0.79 ± 0.05	2.87 ± 0.30	1.79 ± 0.12
1.500	0.67 ± 0.12	2.43 ± 0.24	0.95 ± 0.05
2.000		2.33 ± 0.20	0.82 ± 0.06
2.500		2.04 ± 0.06	0.67 ± 0.03
3.000		1.67 ± 0.06	0.68 ± 0.05
		He^{2+} Projectile	
0.500			2.09 ± 0.13
1.000			1.07 ± 0.04
1.500			0.76 ± 0.09

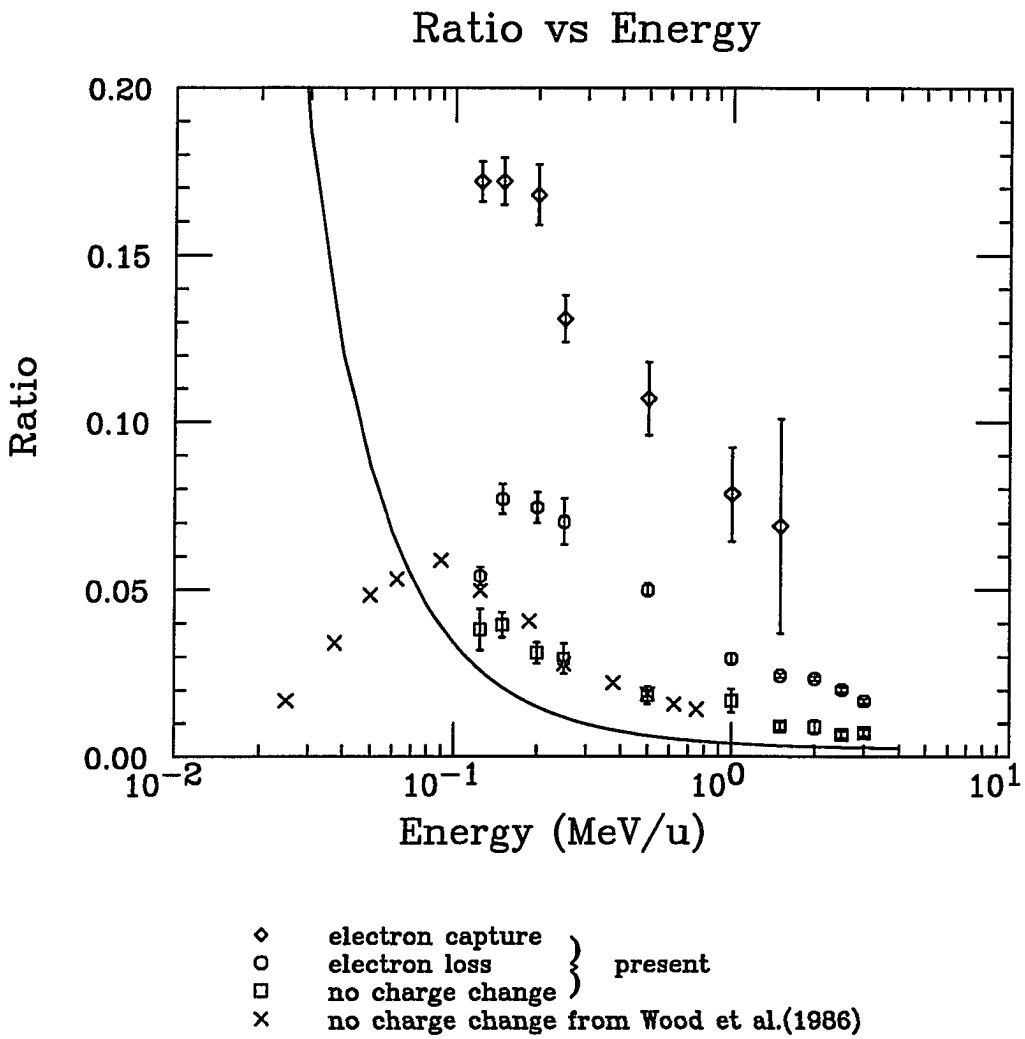

Figure 15. Ratios as a Function of Projectile Energy for Double-to-Single Ionization of Helium By He^+ Ions Undergoing Electron Capture, Electron Loss, and No Charge Change.

The solid curve represents the empirical scaling (Eq. 20) of Knudsen et al. for q=1 projectiles (1984).

region only (Figure 16b). As shown in Fig. 16a, the present results for He^{2+} projectiles are in rather good agreement with those from Andersen et al. (1986), and with the empirical scaling of Knudsen et al. (solid line). For He^{+} projectiles, however, the predicted linear relationship between the ratio and the scaled energy is not evident over the full energy range investigated. But when the same results are plotted in Fig. 16b for only the high energy region, a clear linearity is displayed. In order to find the high energy limits for electron capture, electron loss and no charge change, a linear least-squares fit was applied to the data as indicated by the dashed lines in Fig. 16b. The y-intercepts for these dashed lines associated with electron capture, electron loss and no charge change are, respectively, 0.056, 0.015, 0.0063. The solid line, with the y-intercept being 0.0022, represents the empirical scaling of Knudsen et al. (1984) for fully stripped ions. Obviously, the asymptotic high-energy limits (the y-intercepts in the graph) are different for the different outgoing projectile charge states and are all higher than the predicted shakeoff limit of R=0.0022 for fully stripped projectiles. Again, these results indicate that the high-energy limit is strongly dependent on the average impact parameter of the collision. As proposed by Knudsen et al. (1987), the high-energy limit of the ratio associated with projectile electron capture is 0.058 (refer to Eq. 21). The present deduced ratio for electron capture in the high-energy limit by He^{+} ions is 0.056, which is very close to the value obtained by Knudsen et al. (1987). The present ratio in the high-energy limit for pure ionization of helium by He^{+} projectiles (= 0.0063), however, is almost three times larger than that obtained for fully stripped ions (= 0.0022). The fact that the He^{+} results are so much different from the He^{2+} results and from results for other fully stripped ions indicates that the extra electron in the He^{+} projectile might be significantly involved in the collision interaction.

The high energy limits of the ratios, together with that for photoionization and

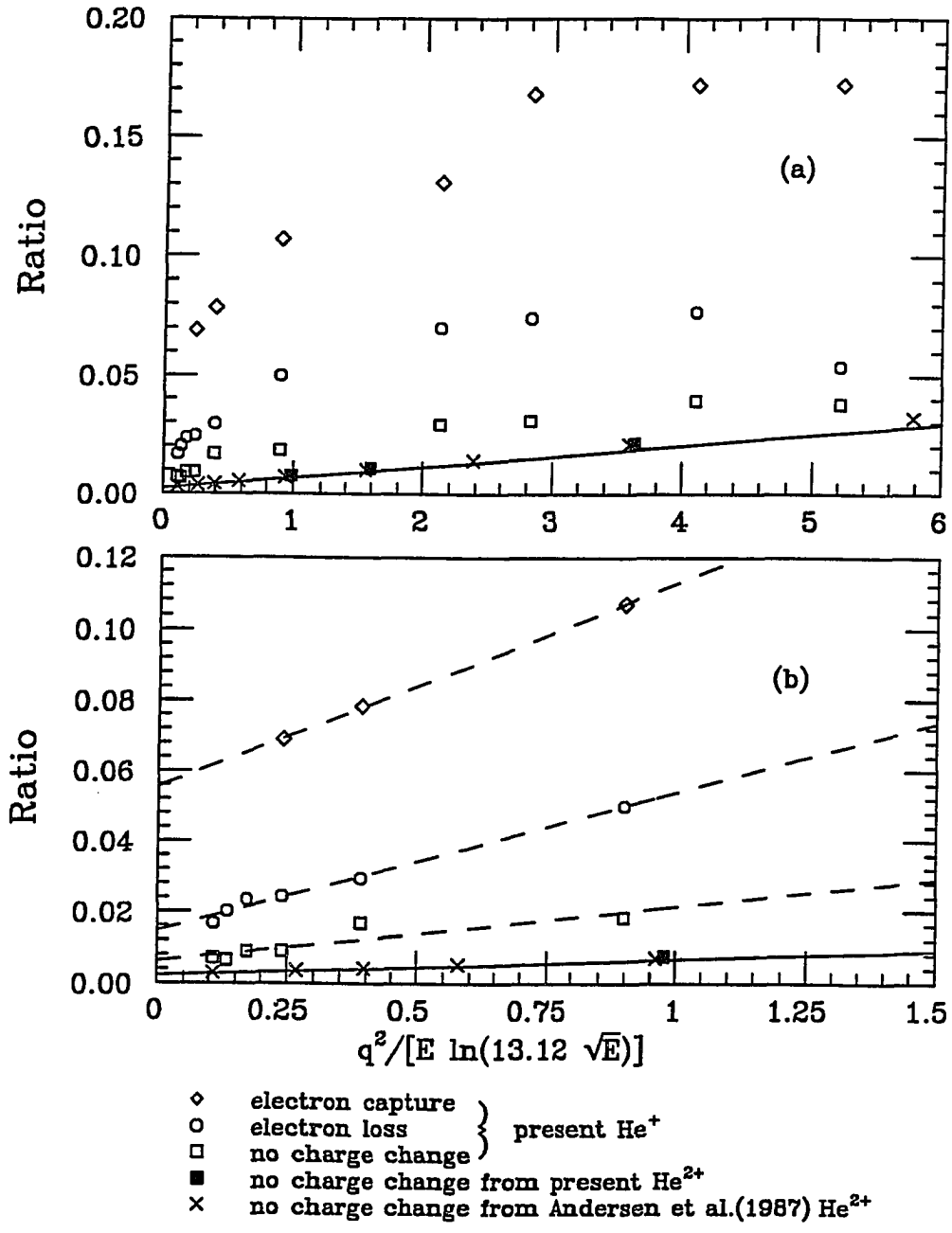

Figure 16. Ratios as a Function of Scaled Projectile Energy.

(a) For the full energy range investigated; (b) high-energy portion. The dashed lines are least-squares fits to the present He^+ data shown in the figure, and the solid line represents the scaling of Knudsen et al. (1984).

Table 6

Experimental High Energy Limits of Ratios of Double-to-Single Ionization Cross Sections in Helium Target

Projectiles	High energy ratio	Reference
Pure ionization by He^+	6.3×10^{-3}	Present
Ionization + capture by He^+	5.6×10^{-2}	Present
Ionization + loss by He^+	1.5×10^{-2}	Present
Pure ionization by He^{2+}	2.7×10^{-3}	Present
Photoionization	3.4×10^{-2}	Schmidt et al., 1976
Ionization by p^+, e^-	2.7×10^{-3}	Knudsen et al., 1984
Ionization by fully stripped ions (empirical)	2.2×10^{-3}	Knudsen et al., 1984
Ionization by N^{7+}	1×10^{-2}	Heber et al., 1990

those for various projectiles are listed in Table 6. As can be seen, the high energy limits for fully stripped ions (p^+, He^{2+}) and electrons are basically the same (about 2~3 $\times 10^{-3}$), except for N^{7+} (~ 0.01) which is 4.5 times higher. The reason could be that the energies investigated (10-30 MeV/u) are not in the shakeoff regime. For shakeoff to dominate, we must have $v/q \geq 10$ a.u., while the highest v/q (corresponding to 30 MeV/u) investigated for N^{7+} is only 4.8 a.u., indicating that it is in the TS dominated region. As compared to the high energy limit for photoionization (0.034), the pure ionization ratios by projectiles with or without electrons are all smaller. Furthermore, the pure ionization ratio for He^+ (0.0063) is higher than that for He^{2+} (0.0027), which agrees with the prediction of Wang et al. (1990), i.e., $R_{H^+} \approx R_{He^{2+}} < R_{He^+} < R_{photon}$. However, the high energy limit for He^+ projectiles undergoing electron capture (0.056) is twice as large as that for photons (0.034), but that associated with electron loss (0.015) is only half as large as the photoionization limit. Further investigation is clearly required to determine the connection between the photon and charged particle high energy limits.

In order to further understand the observed difference between He^+ and fully stripped projectiles and present a detailed picture of ionization of helium by partially and fully stripped projectiles, ratios of pure ionization by He^+ ions from the present work and from the work of Wood et al. (1986) are compared with those for various fully stripped ions obtained by different groups (present, He^{2+}; Andersen et al., H^+, He^{2+}, 1987; Shah and Gilbody, H^+, He^{2+}, Li^{3+}, 1985; Heber et al., N^{7+}, 1990; McGuire et al., various projectiles with charge states ranging from 6 to 44, 1987). All these results are plotted as a function of v/q in Figure 17. As can be seen, the present results for He^+ (q=1 is used in Fig. 17) are in good agreement with those from Wood et al. (1986). Results for the various fully stripped projectiles by different groups are, in

general, in reasonable agreement with one another, especially at high v/q values. However, an interesting deviation between the He^+ results and results of fully stripped ions is displayed in Figure 17. For v/q values ranging from 2 to 10 a.u., ratios from both He^+ and fully stripped ions are linear in v/q, but the He^+ ratios are almost twice as large as those for fully stripped ions. This deviation indicates that the electron in the He^+ projectile has participated in the collision interaction, giving rise to a higher probability for double ionization.

As mentioned in Chapter II, the He^+ projectile can be treated as a point-like particle with an effective charge $q_{eff}(b)$ which is dependent on the impact parameter b (Toburen et al., 1981; McGuire et al., 1981). Therefore the charge q should be replaced by q_{eff} in Fig. 17. However, since pure ionization is expected to occur at large average impact parameters, from Eq. (22), $q_{eff} \approx 1$, which is the same as the charge used in Fig. 17. On the other hand, if the observed He^+ data are fitted to the common curve for the fully stripped ions shown in Fig. 17, an effective charge of ~2 is required, inferring that the average impact parameter is small. If we apply the free collision model described in Chapter II, the He^+ ion is equivalent to an electron and a He^{2+} ion. Then the cross sections for He^+ should be the sum of those for e^- and He^{2+}, and the ratio should be:

$$R = \frac{\sigma_{2I}(He^{2+}) + \sigma_{2I}(e^-)}{\sigma_{1I}(He^{2+}) + \sigma_{1I}(e^-)} \qquad (43)$$

The ratios for He^+ (+ symbols), He^{2+} (solid curve), and e^- (× symbols) together with those obtained from Eq. 43 (○ symbols) are plotted as a function of v/q_{eff} in Figure 18. The q_{eff} is 2.24, 2, 1, and 2.24 for He^+, He^{2+}, e^-, and results obtained from free collision model, respectively. The He^+ results shown are from the present work and from Wood et al. (1986). The solid line represents the empirical scaling of

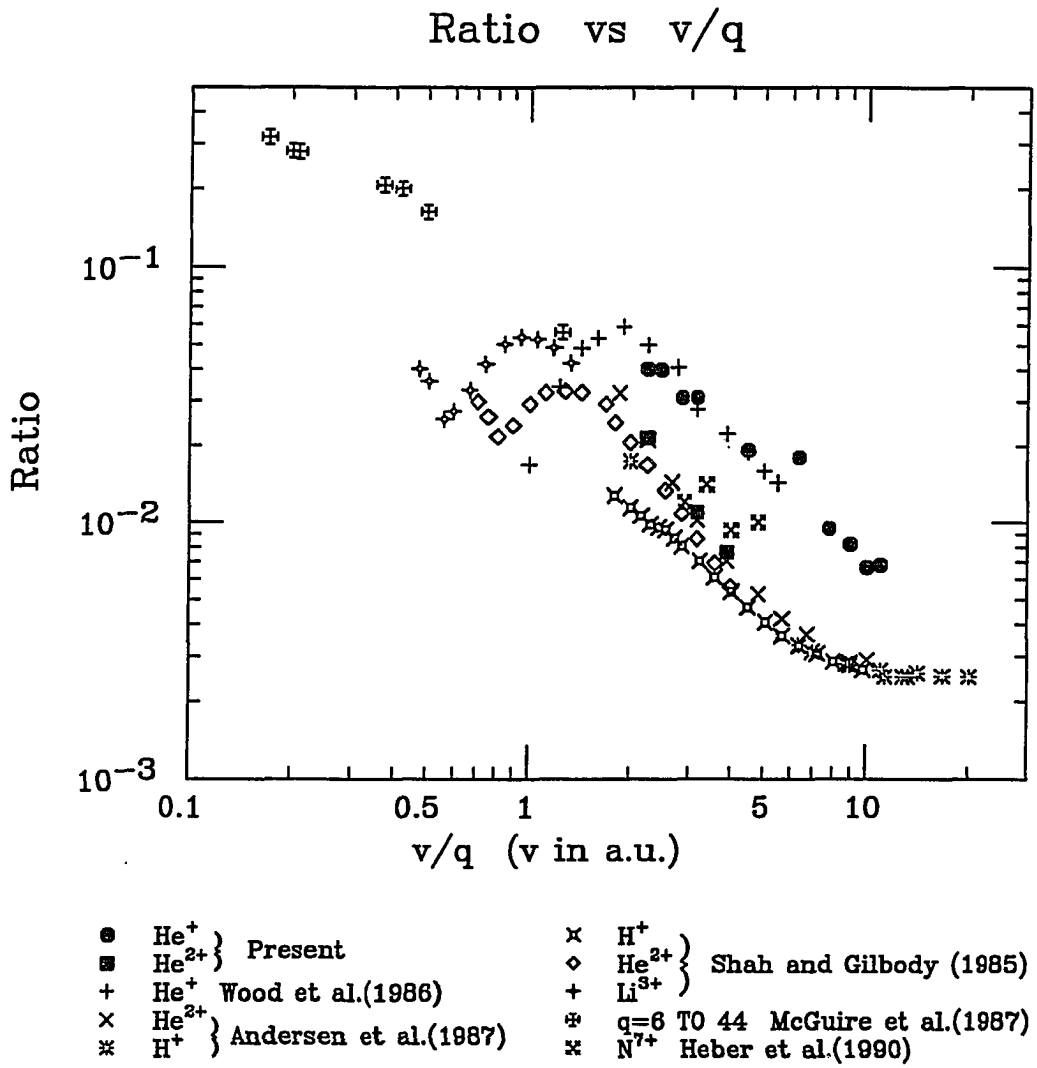

Figure 17. Ratios of Double-to-Single Ionization of Helium as a Function of v/q, where v is the projectile velocity (in atomic units), and q is the projectile charge state.

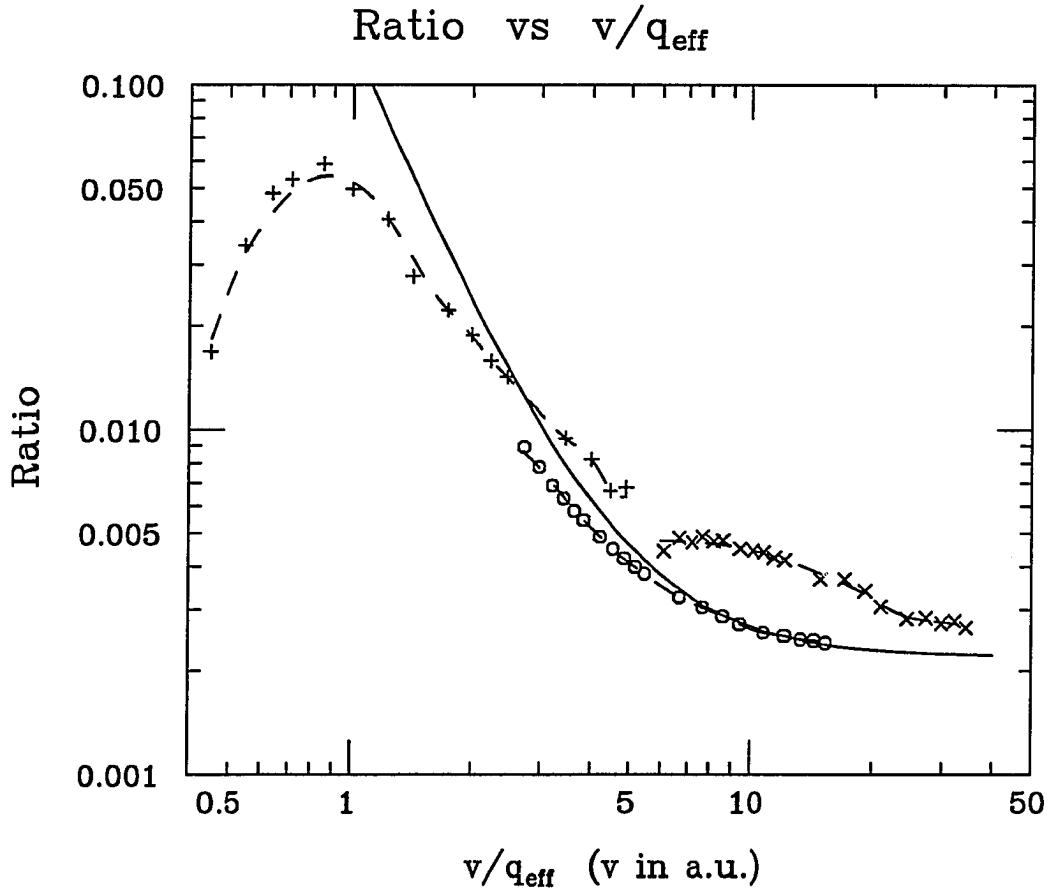

Figure 18. Comparison of the Observed He^+ Ratios With the Ratios Obtained From the Free Collision Model.

The solid line represents the empirical scaling of Knudsen et al. (1984) with q_{eff}=2. The dashed lines are to guide the eye.

Knudsen et al. (1984) for He^{2+}. As seen in Fig. 18, the ratios obtained from the free collision model are in agreement with those for He^{2+} from Knudsen's empirical equation at the highest v/q_{eff} values. However, there is a clear discrepancy between the observed He^{+} ratios and the ratios obtained from free collision model. The reason for this is not clear. One possible explanation for this discrepancy is that the projectile electron is not really weakly bound to the nucleus as required by the free collision model, and thus the He^{+} projectile is not treatable as two independent particles (i.e., He^{2+} and e^{-}). More theoretical considerations are necessary to quantitatively describe this many-body problem. Meanwhile, a future experiment on the double ionization of helium with $Li^{1,2,3+}$ projectiles would likely provide useful additional information on the effect of projectile electron(s) on the double ionization process.

CHAPTER VI

CONCLUSIONS

Double ionization of helium has been investigated in the energy range from 0.125 to 3 MeV/u for He^+ projectiles, and 0.5 to 1.5 MeV/u for He^{2+} projectiles. Singly- and doubly-charged recoiling target ions were detected in coincidence with projectiles undergoing electron capture, electron loss, or no charge change using a recoil time-of-flight spectrometer. The cross sections for single and double ionization of helium associated with capture, loss or no charge change were obtained and compared with various scaling rules. The ratios of double-to-single target ionization were determined for each outgoing projectile charge state. High energy limits of the ratios were compared with the high-energy photoionization ratio. Ratios of pure ionization for He^+ ions were compared with those obtained for fully stripped ions by various groups.

For the lowest energies investigated in the present work, the double-to-single ionization ratios are consistent with the two-step mechanism for double ionization. The present results approach the high-energy limit as evidenced by the fact that the ratios reach nearly constant values for the highest energies investigated. At these highest energies, the ratios for He^{2+} projectiles are in rather good agreement with the shakeoff limit for fully stripped ions predicted by Knudsen et al. (1984), while the ratios for He^+ projectiles are all higher than this shakeoff limit. Furthermore, the high energy limit obtained for He^+ is strongly dependent on the outgoing projectile charge state indicating differing amount of electron correlation being responsible for the double ionization of helium.

As compared with the high energy limit ($R_\gamma = 0.034$) for photoionization, the present double-to-single ionization ratio for He^+ projectiles undergoing electron capture (=0.056) is almost twice as large as R_γ, while that undergoing electron loss (=0.015) is only half as large as R_γ. For pure ionization by He^+, the high energy limit is 0.0063, almost three times as large as that for He^{2+} (0.0027), both of which, however, are much smaller than R_γ. More investigations are necessary to establish a connection in the high energy limit between ionization by charged particles with or without electrons and photoionization.

The ratios (as a function of v/q) for partially stripped projectiles (He^+) are compared with those for various fully stripped projectiles. An interesting deviation is displayed, indicating that the electron in the He^+ projectile might be significantly involved in the collision interaction, giving rise to a higher probability for double ionization. The ratio of double-to-single ionization calculated from free collision model is compared with the measured ratio for He^+ projectiles, and there is a discrepancy between them.

A future experiment with projectile velocities up to $\sim 40 v_{Bohr}$ would be useful in determining the double-to-single ionization ratio in the high velocity limit for He^+ ions, therefore giving rise to a better understanding of the effect of the projectile electron on the ionization process. Furthermore, investigations of the double ionization of helium by other partially stripped ions (e.g., $Li^{1,2+}$) or neutral atoms (e.g., He^0, Li^0) would provide more information about the effect of the projectile electrons on the double ionization process. Meanwhile, theoretical studies are necessary to determine the dependence of $q_{eff}(b)$ on the impact parameter, and therefore help to understand the influence of the projectile electron on the ionization interactions.

BIBLIOGRAPHY

Andersen, L. H., Hvelplund, P., Knudsen, H., Moller, S. P., Elsener, K., Rensfelt, K. G., & Uggerhoj, E. (1986). Single and double ionization of helium by fast antiproton and proton impact. Physical Review Letters, 57, 2147.

Andersen, L. H., Hvelplund, P., Knudsen, H., Moller, S. P., Sorensen, A. H., Elsener, K., Rensfelt, K. G., & Uggerhoj, E. (1987). Multiple ionization of He, Ne, and Ar by fast protons and antiprotons. Physical Review A, 36, 3612.

Barnett, C. F., Hunter, H. T., Kirkpatrick, M. I., Alvarez, I., Cisneros, C., & Phaneuf, R. A. Collisions of H, H_2, He and Li atoms and ions with atoms and molecules. In "Atomic Data for Fusion," Oak Ridge National Laboratory Report, No. ORNL-6086, Vol. 1, 1990.

Bohr, N. (1948). K. Dansk. Vidensk. Selsk. Mat. Fys. Meddr. 18, No. 8.

Boman, S. A. (1988). Single-electron capture and loss cross sections vs. target Z for 1 MeV/u oxygen ions incident on gases. Master's thesis (Western Michigan University, Kalamazoo)

Boman, S. A., Bernstein, E. M., & Tanis, J. A. (1989). Single-electron capture and loss cross sections versus target Z for 1 MeV/u oxygen ions incident on gases. Physical Review A, 39, 4423.

Byron, F. W., Jr., & Joachain, C. J. (1966). Importance of correlation effects in the ionization of helium by electron impact. Physical Review Letters, 16, 1139.

Drawin, H. W. (1980). Atomic and molecular structure and collision data with application to fusion research. In Invited lectures and progress reports of SPIG-78, Dubrovnik, Yugloslavia, Aug. 28 - Sep. 2 1978 (pp. 633-659). Beograd, Yugloslavia: Institute of Physics.

DuBois, R. D. & Manson, S. T. (1986). Coincidence study of doubly differential cross sections: Projectile ionization in He^+ -He collisions. Physical Review Letters, 57, 1130.

DuBois, R. D., & Toburen, L. H. (1988). Single and double ionization of helium by neutral-particle to fully stripped ion impact. Physical Review A, 38, 3960.

Edwards, A. K., Wood, R. M., & Ezell, R. L. (1985). Double ionization of helium by He^+ projectiles. Physical Review A, 32, 1346.

Haugen, H. K., Andersen, L. H., Hvelplund, P., & Knudsen, H. (1982). Multiple ionization of noble gases by fully stripped ions. Physical Review A, 26, 1962.

Heber, O., Bandong, B. B., Sampoll, G., & Watson, R. L. (1990). Double and single ionization of helium by high-velocity N^{7+} ions. Physical Review Letters, 64, 851.

Horsdal Pedersen, E. & Larsen, L. (1979). Simultaneous ionisation of both collision partners in single collisions between H projectiles and He and Xe targets. Journal of Physics B, 12, 4099.

Inokuti, M. (1971). Inelastic collisions of fast charged particles with atoms and molecules—the Bethe theory revisited. Reviews of Modern Physics, 43, 297.

Knudsen, H., Andersen, L. H., Hvelplund, P., Astner, G., Cederquist, H., Danared,H., Liljeby, L., & Rensfelt, K-G. (1984). An experimental investigation of double ionisation of helium atoms in collision with fast, fully stripped ions. Journal of Physics B, 17, 3545.

Knudsen, H., Andersen, L. H., Hvelplund, P., Sorensen, J., & Ciric, D. (1987). Simultaneous capture and ionisation for fast ion impact on helium. Journal of Physics B, 20, L253.

Knudsen, H., Haugen, H. K., & Hvelplund, P. (1981). Single-electron-capture cross section for medium- and high-velocity, high charged ions colliding with atoms. Physical Review A, 23, 597.

Madison, D. H., & Merzbacher, E. (1972). Theory of charged-particle excitation. In B. Crasemenn (Ed.), Atomic inner-shell processes (pp. 1-72). New York, Academic.

McGuire, J. H. (1982). Double ionization of helium by protons and electrons at high velocities. Physical Review Letters, 49, 1153.

McGuire, J. H. (1984). High-velocity limits for the ratio of double to single ionisation by charged particles and by photons. Journal of Physics B, 17, L779.

McGuire, J. H. (1987). Correlation in atomic scattering. Physical Review A, 36, 1114.

McGuire, J. H., Muller, A., Schuch, B., Groh, W., & Salzborn, E. (1987). Ionization of helium by highly charged ions at 1.4 MeV/amu. Physical Review A, 35, 2479.

McGuire, J. H., Salzborn, E., & Muller, A. (1987). Simultaneous capture and ionization in helium. Physical Review A, 35, 3265.

McGuire, J. H., Stolterfoht, N., & Simony, P. R. (1981). Screening and antiscreening by projectile electrons in high-velocity atomic collisions. Physical Review A, 24,97.

McGuire, J. H., & Weaver, O. L. (1977). Independent electron approximation for atomic scattering by heavy particles. Physical Review A, 16, 41.

McKenzie, M. L., & Olson, R. E. (1987). Ionization and charge exchange in multiply-charged-ion — helium collisions at intermediate energies. Physical Review A, 35, 2863.

Mittleman, M. H. (1966). Single and double ionization of He by electrons. Physical Review Letters, 16, 498.

Ramsey, N. F. (1956). Molecular beams. Oxford: Clarendon.

Reading, J. F., & Ford, A. L. (1987). Double ionization of helium by protons and antiprotons in the energy range 0.30 to 40 MeV. Physical Review Letters, 58, 543.

Schlachter, A. S., Stearns, J. W., Berkner, K. H., Stockli, M. P., Graham, W. G., Bernstein, E. M., Clark, M. W., & Tanis, J. A. (1987). Electron capture for fast highly charged ions in He: An empirical scaling rule revisited. In XV International Conference on the Physics of Electronic and Atomic Collisions (pp. 505-506). Belfast, United Kingdom: International ICPEAC Organization.

Schlachter, A. S., Stearns, J. W., Graham, W. G., Berkner, K. H., Pyle, R. V., & Tanis, J. A. (1983). Electron capture for fast highly charged ions in gas targets: An empirical scaling rule. Physical Review A, 27, 3372.

Schmidt, V., Sandner, N., Kuntzemuller, H., Dhez, P., Wuilleumier, F., & Kallne, E. (1976). Double ionization of rare gases. II. Ion formation by photon impact. Physical Review A, 13, 1748.

Schram, B. L., Boerboom, A. J. H., & Kistemaker, J. (1966). Partial ionization cross sections of noble gases for electrons with energy 0.5-16 keV. Physica 32, 185.

Shah, M. B., & Gilbody, H. B. (1985). Single and double ionisation of helium by H^+, He^{2+} and Li^{3+} ions. Journal of Physics B, 18, 899.

Sidorovitch, V. A., & Nikolaev, V. S. (1983). Ionisation of He atoms by H^+, He^{2+}, Li^{3+} nuclei. Journal of Physics B, 16, 3243.

Steigman, G. (1975). Charge transfer reactions in multiply charged ion-atom collisions. Astrophysical Journal, 199, 642.

Tanis, J. A. (1989). Interactions involving two electrons in ion-atom collisions. Nuclear Instruments and Methods in Physics Research, B40/41, 70.

Tanis, J. A., Bernstein, E. M., Clark, M. W., Ferguson, S. M., and Price, R. N. (1991). Target ionization accompanied by projectile electron loss in fast $O^{6,7+}$ + He collisions. Physical Review A, 43, 4723.

Tanis, J. A., Bernstein, E. M., Clark, M. W., Ferguson, S. M., Price, R. N., & Woodland, W. (1989). Transfer ionization in ion collisions with helium. Nuclear Instruments and Methods in Physics Research, B42, 523.

Tanis, J. A., Clark, M. W., Price, R., & Olson, R. E. (1987). Contribution of transfer ionization to total electron capture from a helium target. Physical Review A, 36, 1952.

Tanis, J. A., Schiwietz, G., Schneider, D., Stolterfoht, N., Graham, W. G., Altevogt, H., Kowallik, R., Mattis, A., Skogvall, B., Schneider, T., & Szmola, E. (1989). Evidence for electron correlation during double capture in fast ($v \sim 10$ a.u.) collisions. Physical Review A, 39, 1571.

Toburen, L. H., Stolterfolt, N., Ziem, P., & Schneider, D. (1981). Electronic screening in heavy-ion—atom collisions. Physical Review A, 24, 1741.

Wang, L. J., King, M., & Morgan, T. J. (1986). Fast Rydberg hydrogen atom collisions with neutral atoms and molecules. Journal of Physics B, 19, L623.

Wang, Y. D., Straton, J. C., McGuire, J. H., & DuBois, R. D. (1990). High-velocity limits for the ratio of double to single ionisation of helium by projectiles with electrons. Journal of Physics B, 23, L133.

Wood, R. M., Edwards, A. K., & Ezell, R. L. (1986). Cross sections for the single and double ionization of helium by He^+ projectiles. Physical Review A, 34, 4415.